

Key Points:

- Both surface roughness and stability changes from sea ice loss drive the sign and magnitude of projected Arctic wind speed trends
- Changing surface roughness does not drive significant coupled feedbacks that impact Arctic sea ice mean state and trends
- Decreasing surface roughness from ice loss modestly impacts surface momentum fluxes but turbulent heat flux impacts are insignificant

Supporting Information:

Supporting Information may be found in the online version of this article.

Correspondence to:

A. K. DuVivier,
duvivier@ucar.edu

Citation:

DuVivier, A. K., Vavrus, S. J., Holland, M. M., Landrum, L., Shields, C. A., & Thaker, R. (2023). Investigating future Arctic sea ice loss and near-surface wind speed changes related to surface roughness using the Community Earth System Model. *Journal of Geophysical Research: Atmospheres*, 128, e2023JD038824. <https://doi.org/10.1029/2023JD038824>

Received 4 MAR 2023
Accepted 10 SEP 2023

Author Contributions:

Conceptualization: Alice K. DuVivier, Stephen J. Vavrus, Marika M. Holland, Laura Landrum, Christine A. Shields, Rudradutt Thaker

Data curation: Alice K. DuVivier

Formal analysis: Alice K. DuVivier, Stephen J. Vavrus, Marika M. Holland

Funding acquisition: Stephen J. Vavrus, Laura Landrum

Investigation: Alice K. DuVivier

Project Administration: Stephen J. Vavrus, Laura Landrum

Validation: Alice K. DuVivier

© 2023. The Authors.

This is an open access article under the terms of the [Creative Commons Attribution -NoDerivs License](#), which permits use and distribution in any medium, provided the original work is properly cited and no modifications or adaptations are made.

Investigating Future Arctic Sea Ice Loss and Near-Surface Wind Speed Changes Related to Surface Roughness Using the Community Earth System Model

Alice K. DuVivier¹ , Stephen J. Vavrus^{2,3} , Marika M. Holland¹ , Laura Landrum¹ , Christine A. Shields¹ , and Rudradutt Thaker^{2,4}

¹Climate and Global Dynamics, National Center for Atmospheric Research, Boulder, CO, USA, ²Nelson Institute Center for Climatic Research, University of Wisconsin, Madison, WI, USA, ³Wisconsin State Climatology Office, Madison, WI, USA,

⁴Department of Atmospheric and Oceanic Sciences, University of Wisconsin, Madison, WI, USA

Abstract The Arctic is undergoing a pronounced and rapid transformation in response to changing greenhouse gasses, including reduction in sea ice extent and thickness. There are also projected increases in near-surface Arctic wind. This study addresses how the winds trends may be driven by changing surface roughness and/or stability in different Arctic regions and seasons, something that has not yet been thoroughly investigated. We analyze 50 experiments from the Community Earth System Model Version 2 (CESM2) Large Ensemble and five experiments using CESM2 with an artificially decreased sea ice roughness to match that of the open ocean. We find that with a smoother surface there are higher mean wind speeds and slower mean ice speeds in the autumn, winter, and spring. The artificially reduced surface roughness also strongly impacts the wind speed trends in autumn and winter, and we find that atmospheric stability changes are also important contributors to driving wind trends in both experiments. In contrast to the clear impacts on winds, the sea ice mean state and trends are statistically indistinguishable, suggesting that near-surface winds are not major drivers of Arctic sea ice loss. Two major results of this work are: (a) the near-surface wind trends are driven by changes in both surface roughness and near-surface atmospheric stability that are themselves changing from sea ice loss, and (b) the sea ice mean state and trends are driven by the overall warming trend due to increasing greenhouse gas emissions and not significantly impacted by coupled feedbacks with the surface winds.

Plain Language Summary This study uses coupled Earth system model experiments to investigate how changes in near-surface winds in the Arctic may be driven by changing surface roughness and/or stability in different regions and seasons. We find that the near-surface wind mean state and future trends are driven by changes in both surface roughness and atmospheric stability that are changing due to sea ice loss. In contrast, the sea ice mean state and trends are primarily driven by overall warming trends and not significantly impacted by coupled interactions with the surface winds. Our study results are important because they show that sea ice loss is driving future change in meteorological near-surface conditions that can impact vessel-based transportation in the Arctic.

1. Introduction

The Arctic is undergoing dramatic changes in response to rising temperatures from increases in global greenhouse gasses. Some of the most dramatic observed changes have been the decline in sea ice extent and volume over the past several decades (Kwok, 2018; Meier et al., 2022) and the increasing Arctic wind speeds over the historical period (Jakobson et al., 2019; Redilla et al., 2019; Stegall & Zhang, 2012). In future decades, sea ice is projected to decrease and the Arctic will become seasonally ice free (e.g., DeRepentigny et al., 2020; Jahn et al., 2016; Notz & Community, 2020). Models also project that near-surface wind speeds are likely to get higher in the Arctic (e.g., Alkama et al., 2020; Knippertz et al., 2000; McInnes et al., 2011; Mioduszewski et al., 2018; Vavrus & Alkama, 2021).

The combination of sea ice loss with increasing winds has important implications for people in the Arctic. Sea ice loss has expanded marine access for larger vessels (Melia et al., 2016; Stevenson et al., 2019), and the combination of more open water with stronger winds has led to larger wave heights in the Arctic in the recent past due to increased fetch without sea ice cover (Wang et al., 2015; Waseda et al., 2018). Indeed, projections using coupled ocean-wave models indicate future increases in significant wave heights in the Arctic, though there is relatively

Writing – original draft: Alice K. DuVivier, Stephen J. Vavrus, Marika M. Holland, Laura Landrum, Christine A. Shields, Rudradutt Thaker

large variability in the wave field (Dobrynin et al., 2012; Khon et al., 2014). Larger waves will impact both large vessels as well as smaller boats, leading, e.g., to a decreasing frequency of subsistence whale hunting activities (Ashjian et al., 2010). Additionally, larger waves, especially during cyclones, contribute to severe coastal erosion that threatens human settlements (Barnhart et al., 2014). Therefore, it is particularly important to fully understand the relationships between sea ice loss and near-surface winds due to the large human and physical system impacts.

Multiple studies of coupled model projections using different model configurations and forcing scenarios indicate that in the Arctic near-surface wind speeds are likely to get higher particularly in autumn and winter (e.g., Alkama et al., 2020; Knippertz et al., 2000; McInnes et al., 2011; Mioduszewski et al., 2018; Schneider et al., 2022; Vavrus & Alkama, 2021; Yu et al., 2020). Early global studies did not focus on causes for the Arctic change (Dobrynin et al., 2012; McInnes et al., 2011), and some early Arctic-focused studies identified a likely relationship between sea ice loss and winds but did not investigate the mechanisms further (Aksenov et al., 2016; Khon et al., 2014). Winds are caused by large scale atmospheric pressure gradients that drive geostrophic winds, which are modified by turbulent transfer of momentum. Thus, there are three possible drivers of increasing Arctic near-surface winds. First, tightening of atmospheric pressure gradients due to changes in circulation could increase geostrophic wind speeds. Recent studies show that across a variety of coupled models pressure gradients and the resulting impact on geostrophic wind speed are largely insignificant and therefore not a primary driver of near-surface wind change (Mioduszewski et al., 2018; Ruosteenoja et al., 2019; Vavrus & Alkama, 2021). Second, reduced atmospheric stability due to enhanced surface warming as sea ice melts (Kay et al., 2011) could lead to enhanced turbulent transport from the free troposphere downward (Jakobson et al., 2019; Knippertz et al., 2000; Ruosteenoja et al., 2019; Seo & Yang, 2013). Third, reduction in surface roughness due to the transition from sea ice cover to open ocean could lead to an acceleration of near-surface winds (Knippertz et al., 2000; Martin et al., 2014).

The relative contribution of the stability and surface roughness to the wind speed increases is still unclear. Additionally, the relationships between changing winds and sea ice as both drivers of and responders to regional climate change are not well understood. Strengthening of the poleward near-surface wind component has been found to enhance the poleward moisture and heat flux that may boost sea ice loss (Alkama et al., 2020). Additionally, increasing near-surface wind speeds could initiate feedbacks related to ocean mixing and/or ice transport that could impact sea ice loss. Therefore, this manuscript aims to answer the following two questions:

1. What are the relative contributions of changing surface roughness and boundary layer stability to the projected increasing wind speeds?
2. Does changing surface roughness have any coupled impacts that contribute to Arctic sea ice loss or affect turbulent fluxes?

To answer these questions, we modify the sea ice roughness in an earth system model to artificially reduce sea ice roughness so it is comparable to ocean values, and thereby remove the trend in surface roughness over the 21st century that would normally accompany sea ice loss. We compare these perturbed experiments to a large initial condition ensemble as a control. While our results rely on only one model, we are able to quantify the impact of the changing surface roughness on Arctic wind speed mean state and trends and coupled processes.

2. Data and Methods

2.1. Model Experiments

This study uses the Community Earth System Model Version 2 (CESM2) (Danabasoglu et al., 2020). As control experiments, we analyze 50 members of the CESM2 Large Ensemble (CESM2-LE) that use standard Coupled Model Intercomparison Project Phase 6 (CMIP6) historical forcing (1850–2014) and SSP3-7.0 forcing for future experiments (2015–2100) (Rodgers et al., 2021). All model experiments use the same standard model configuration that is described in detail in Danabasoglu et al. (2020) and Rodgers et al. (2021). All components are at nominal 1° resolution, and the ice and ocean models share a model grid that has uniform zonal spacing but varying meridional spacing. The CESM2 atmospheric component is Community Atmosphere Model version 6 (CAM6), which has 32 vertical levels, and the ocean component is the Parallel Ocean Program version 2 (POP2), which has 60 vertical levels. CESM2 uses the CICE version 5 (CICE5) thermodynamic-dynamic sea ice model (Hunke et al., 2015). The surface fluxes are calculated in the surface model (CICE5 or POP2 for ocean points) and passed through a coupler to the atmosphere model (CAM6). In CESM2, CICE5 has an ice thickness distribution (five categories), prognostic sea ice salinity, and salinity dependent freezing temperature (Assur, 1958).

The parameterization of roughness in CESM2 is simple and set to a constant (see Section 2.2), and ice keel and sail heights are not explicitly modeled. Arctic sea ice in CESM2 has been validated by multiple studies in terms of ice extent and area, and seasonal cycle (e.g., DeRepentigny et al., 2020; A. K. DuVivier et al., 2020; Webster et al., 2021).

To test the degree to which changing surface aerodynamic roughness and therefore the air-ice drag coefficient influences near-surface wind trends, we performed fully coupled experiments with the same model configuration and forcing as the CESM2-LE but artificially reduced, for the most typical range of wind speeds, the Arctic sea ice roughness such that it is comparable to ocean values. We refer to these experiments as SMOOTH in this manuscript and describe the modified equations in Section 2.2. These experiments utilize the CESM model as a virtual laboratory to better understand feedbacks and processes if surface roughness conditions do not vary in time. The SMOOTH experiments were performed as follows. A single SMOOTH ensemble member with the code change described below was branched from the CESM2-LE control experiment on 1 January 1940 and allowed to freely evolve until 31 December 2014 when CMIP6 historical forcing ends. By completing a 65 year historical model integration, we allow mean state changes originating from the smoothing over sea ice to equilibrate. Then on 1 January 2015 we branched five SMOOTH ensemble members from the historical SMOOTH experiment. All five members use the same model code and external forcing, but we provided a random microperturbation (10^{-14}) to initial atmospheric temperatures. After applying this round-off level perturbation, each ensemble member evolves freely under the same SSP3-7.0 forcing as the CESM2-LE until 2100. All analysis presented in this manuscript uses data from the five ensembles from 2015 to 2100, the period after the historical spin-up was completed. Applying surface smoothing over sea ice results in neutral drag coefficients roughly 50%–60% lower than would otherwise be found over sea ice for wind speeds below 20 m s^{-1} (Figure 1). We perform our analysis in this study over the future period (2020–2100) where we have multiple ensemble members available. Due to the difference in ensemble sizes (CESM2-LE— $n = 50$; SMOOTH— $n = 5$) there is more variability expected in the ensemble mean from SMOOTH as compared to CESM2-LE. Thus, when comparing area mean time series we use bootstrapping, or random resampling to generate statistics as described in Kay et al. (2022), to statistically assess when the SMOOTH ensemble members are different from CESM2-LE. For this study, we focus on the central Arctic (blue shaded region in Figure 1d) and we define seasons based on the sea ice annual cycle. The sea ice growth season is autumn (October, November, December) and winter (January, February, March) while the sea ice melt season is spring (April, May, June), and summer (July, August, September).

2.2. CESM2 Code Modification

Here, we detail the modification we make to the CESM2 model code to artificially smooth the Arctic sea ice. We applied the smoothing only to the Arctic to ensure minimal impacts elsewhere around the globe. Surface roughness is not directly passed to the atmosphere model in CESM2, but it is used to calculate turbulent fluxes that are passed to the atmosphere model through a coupler. To fully understand how the changes in surface roughness would impact coupled surface exchanges, we also describe the turbulent momentum and heat flux calculations in CICE. It is important to note that the treatment of turbulent transfer in CESM2, as well as other Earth system models, is much simpler than in reality. However, because these simple formulations are so widely used in models used for climate projections they are worth investigating.

We modify only the neutral drag coefficient between the ice and atmosphere in the atmospheric boundary layer routine in CICE. The default neutral drag coefficient over sea ice is a constant and calculated as follows:

$$Cd n_{ice} = \left(\frac{\kappa}{\log\left(\frac{z_{ref}}{z_0}\right)} \right)^2 \quad (1)$$

where $\kappa = 0.4$ is the von Karman constant, z_{ref} is the reference height above the surface (10 m), and z_0 is a constant ice roughness length (0.0005 m). In contrast, the neutral drag coefficient over open ocean uses the empirically derived wind speed dependent equation from Large and Yeager (2009)

$$Cd n_{ocn} = \frac{0.0027}{U_{atm}} + 0.000142 + (0.0000764 * U_{atm}) \quad (2)$$

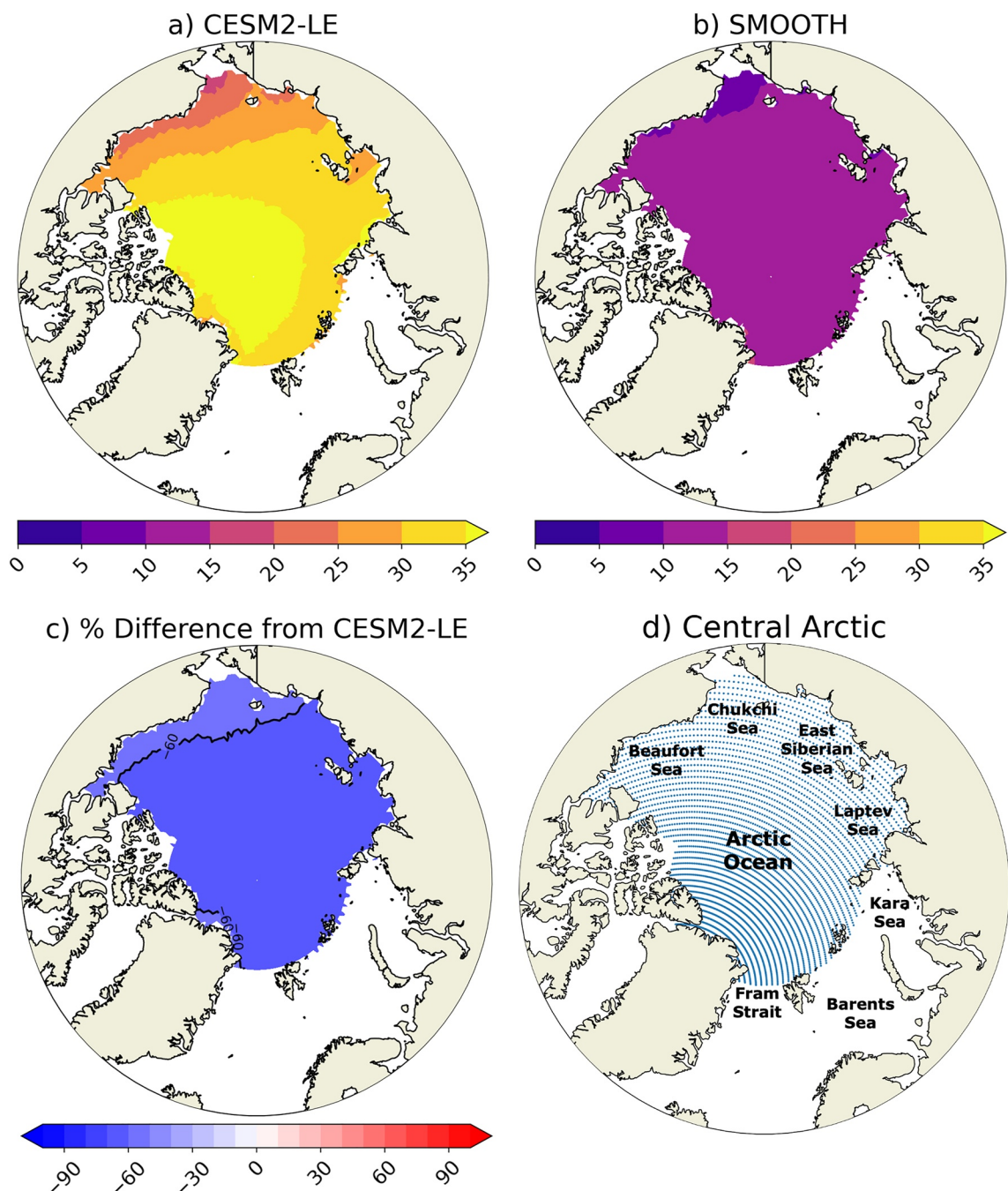


Figure 1. March 2015–2019 mean sea ice-air drag coefficient (unitless) in the central Arctic over areas with sea ice concentrations above 15% for (a) CESM2-LE and (b) SMOOTH, and (c) percent difference of SMOOTH from CESM2-LE. Panel (d) shows the central Arctic region used for this study shaded in blue.

where U_{atm} is the near-surface wind speed from the atmosphere model. The resulting neutral drag coefficients for ice and ocean are shown in Figure 2. In the SMOOTH experiments instead of using the constant neutral drag coefficient (Equation 1), we use the equation for the neutral drag coefficient over ocean (Equation 2). Modifying this single equation is the only change we make to the CICE model code for the SMOOTH experiments.

The purpose of the SMOOTH experiments is to better understand the sensitivity of the change in roughness that occurs with the transition from ice-covered to open ocean conditions. Thus, we are not applying the open ocean equation because it is physically realistic, but we use it to implement conditions in which there is no trend in surface roughness as the surface conditions change due to changing sea ice fraction. For the CESM2-LE experiments,

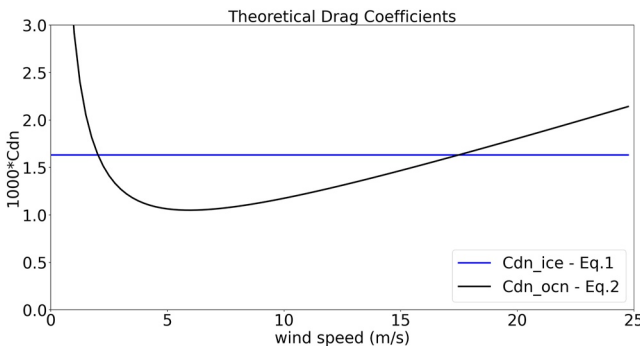


Figure 2. Drag coefficient over ocean (black) and sea ice (blue) for wind speeds between 0 and 25 m s⁻¹ from Equations 1 and 2.

generally speaking, we expect a negative trend in surface roughness over the 21st century as the sea ice retreats and the surface is more frequently open ocean. In the SMOOTH experiments, using Equation 2 removes the connection between the changing sea ice surface conditions since all ocean points, even those with any level of sea ice coverage, will use the same formulation to calculate the neutral drag coefficient throughout the entirety of the simulation. It is important to note that the neutral drag coefficient over water is only smaller than the constant value over ice for wind speeds between ~ 2 and 17.5 m s⁻¹; however, as we can see from Figure 1, the overall effect in the SMOOTH experiments is to reduce the surface drag.

In CICE, the drag coefficient (Cd) used for turbulent fluxes is calculated as

$$Cd = \frac{Cdn}{\left[1 + \left(\frac{rdn}{\kappa} * \psi\right)\right]^2} \quad (3)$$

where Cdn is the neutral drag coefficient (Equations 1 or 2), rdn is the square root of the neutral drag coefficient, κ is the von Karman constant, and ψ is a function that corrects for atmospheric stability. Multiple parameterizations of ψ are available, but we use the default option within CICE5 (Hunke et al., 2015), and in the CICE scheme, changing the surface drag coefficient does not directly affect calculation of ψ . However, decreasing surface roughness will indirectly impact ψ since the roughness length will impact fluxes, which then impacts the Obukhov length, which impacts ψ . It is important to note that heterogeneity in surface sea ice conditions from melt ponds are considered only for the radiation calculations in CICE and do not impact the surface roughness. This is consistent with other CMIP6 models (e.g., Keen et al., 2021; Lecomte et al., 2015; Rousset et al., 2015).

The drag coefficient (Equation 3) is used to calculate turbulent fluxes that are passed to the atmosphere model. In CICE surface stress is calculated as

$$\tau = \rho_{atm} * Cd * (U_{atm} - U_{sfc})^2 \quad (4)$$

where ρ_{atm} is the air density, Cd is calculated using Equation 3, U_{atm} is the scalar wind speed, and U_{sfc} is the surface ice speed. We can assume that the air density remains approximately constant and that the atmospheric wind speeds are much larger than surface ice drift speeds. Therefore, changes in wind stress primarily depend on changes in the surface drag or changes in the wind speed. For the same wind speed and atmospheric stability, a smoother surface leads to smaller drag coefficient and lower surface stress than would occur over a rougher surface. We analyze the total turbulent surface heat flux, which is the sum of the latent and sensible heat fluxes. The sensible heat flux can be written as

$$F_{sens} = \rho_{atm} * C_p * C_H * U_{atm} * (T_{sfc} - T_{air}) \quad (5)$$

and the latent heat flux (evaporation) can be written as

$$F_{lat} = \rho_{atm} * L_v * C_E * U_{atm} * (q_{sfc} - q_{air}) \quad (6)$$

where ρ_{atm} is the air density, C_p is the specific heat of air, L_v is the latent heat of vaporization, U_{atm} is the near-surface scalar wind speed from the atmosphere model, $(T_{sfc} - T_{air})$ is the temperature gradient between the surface and atmosphere, $(q_{sfc} - q_{air})$ is the moisture gradient between the surface and atmosphere, and C_H and C_E are stability dependent transfer coefficients that incorporate the neutral drag coefficient calculated using Equation 3. Both these surface fluxes are proportional to the surface drag and the near-surface scalar wind speed. Therefore, all else being identical, differences in roughness or wind speed between CESM2-LE and SMOOTH would be expected to drive differences in these surface turbulent heat fluxes.

3. Results

3.1. Atmospheric Response

Over the central Arctic, the ensemble mean near-surface wind speed in SMOOTH is significantly higher than CESM2-LE by about 0.5 m s⁻¹ during all seasons except summer, and the SMOOTH ensemble mean wind

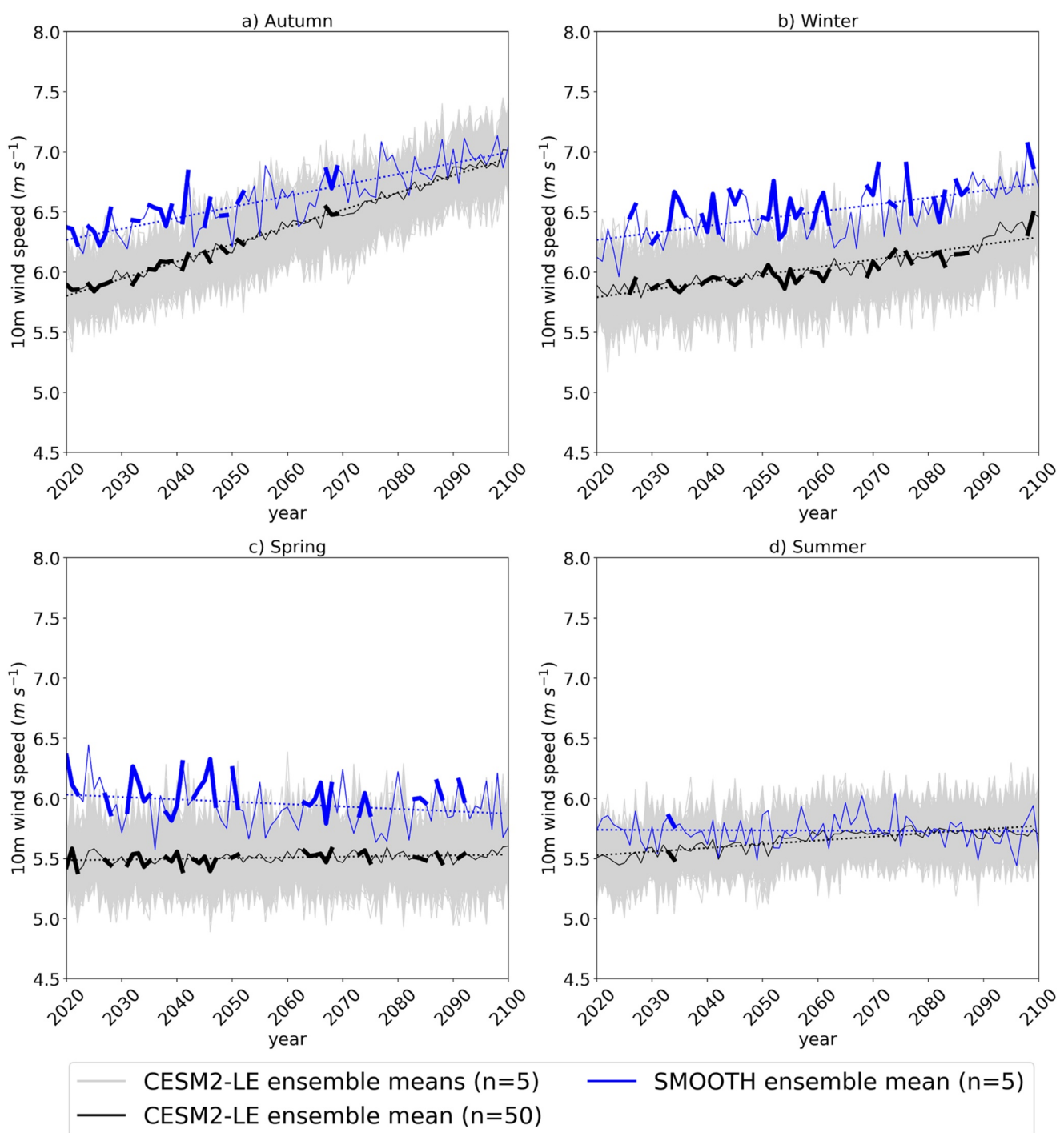


Figure 3. CESM2-LE and SMOOTH time series of central Arctic average 10-m wind speed ($m s^{-1}$) for (a) autumn, (b) winter, (c) spring, and (d) summer. Blue solid lines indicate SMOOTH ensemble mean ($n = 5$), black solid lines indicate CESM2-LE ensemble mean ($n = 50$), and gray solid lines indicate 1,000 CESM2-LE bootstrapped ensemble means ($n = 5$). The blue and black solid lines are thick for years in which the differences are significant at the 95% confidence level. Linear regressions for the ensemble means from 2020 to 2100 are shown as blue and black dashed lines.

speeds are on the high end of the distribution of bootstrapped CESM2-LE means (Figure 3). In summer, the lack of significant wind speed differences between the CESM2-LE and SMOOTH experiments is likely because extensive sea ice melt results in CESM2-LE having comparable surface roughness to SMOOTH (Figure 3d). Previous studies have shown CESM2 simulations have the first ice-free September in the 2020s or 2030s (DeRepentigny et al., 2020), which indicates near-total summertime melt in the central Arctic through the entire

study period, so the surface roughness would be that of open ocean. Autumn is the only season where the mean state differences change systematically during the 21st century from being significantly different in the first half of the 21st century to shrinking in the second half of the 21st century (Figure 3a). The shift in mean wind differences is likely related to the changing sea ice state as the Arctic becomes seasonally ice free and freeze up starts later in autumn. In the early 21st century when there is extensive ice coverage in both experiments, SMOOTH will have roughness of open ocean where CESM2-LE will have a rougher surface. However, later in the century as the open water season increases, the CESM2-LE will have open ocean and a smoother surface, so the SMOOTH mean wind speeds are more similar. In contrast, during winter and spring when there is extensive ice coverage the mean wind differences persist because the roughness differences with ice coverage persist.

Despite the difference in near-surface wind mean state related to a smoother surface, a clear positive trend in wind speeds is evident in both CESM2-LE and SMOOTH during the ice growth seasons, while the trends are much smaller or even slightly negative in the ice melt seasons (Figure 3). The 2020–2100 wind speed trends are positive for both experiments in the ice growth season, but in autumn trend is 38.7% smaller for SMOOTH than the CESM2-LE while in winter the SMOOTH trend is 12.9% smaller than for CESM2-LE (Table 1). In the ice melt season, the SMOOTH wind trends are negative, indicating slowing wind speeds, while the CESM2-LE trends remain positive, though lower magnitude than in the ice growth season. These seasonal differences in wind speed trends suggest that the change in sea ice roughness as ice melts plays a major role in determining the magnitude and sign of the wind trend, although other factors also contribute to drive strengthening winds since SMOOTH has a positive trend in wind speed despite having essentially fixed surface roughness.

The previous analysis used central Arctic mean winds, so to better understand any regional differences we look at spatial maps in ensemble mean wind trends over the central Arctic. During the ice growth seasons, the wind speed trends are positive and significant nearly everywhere for both CESM2-LE and SMOOTH, but the trends are generally 30%–60% smaller in SMOOTH (Figure 4, top and second rows). It is worth noting that SMOOTH has larger trends in the Laptev Sea and north of the Barents Sea, but these are regions where the wind trends are relatively small for both CESM2-LE and SMOOTH so small absolute differences between the simulations appear sizable because of the percent difference calculation. In the ice melt seasons, the wind speed trends for both CESM2-LE and SMOOTH are not significant over large portions of the Arctic, and where the trends are significant the magnitude is much smaller and sometimes opposite sign compared to the ice growth seasons (Figure 4, third and bottom rows). The distribution of significant trends across the central Arctic for both the ensemble means and all individual ensemble members is consistent with these ensemble mean results (Figure S1 in Supporting Information S1). Overall, we find increasing near-surface wind speed trends in both CESM2-LE and SMOOTH during the ice growth season.

Since atmospheric pressure gradients could change geostrophic wind speeds, we investigate whether there are significant differences in the Arctic circulation in CESM2-LE and SMOOTH that could drive the higher near-surface wind speeds in each experiment. In all decades from 2020 to 2100, seasonal differences in the 925 hPa geostrophic wind speed are usually small (<10%), statistically insignificant at the 95% confidence level, and not spatially consistent between decades (Figure 5 and Figure S2 in Supporting Information S1). The sea level pressure contours are also very similar between the two experiments in all seasons. Our results showing minor differences in atmospheric circulation and geostrophic winds are consistent with others who have found that geostrophic wind changes are not the primary driver of near-surface wind changes (Jakobson et al., 2019; Mioduszewski et al., 2018; Ruosteenoja et al., 2019; Vavrus & Alkama, 2021). Thus, geostrophic wind speed differences are not likely to be responsible for the near-surface wind speed mean differences or increasing trends in either CESM2-LE or SMOOTH. Instead, the surface roughness and stability are the major drivers in the mean wind speed and trends, and atmospheric stability will be discussed in more detail in Section 3.4.

3.2. Sea Ice Response

The central Arctic sea ice mean state is very similar in CESM2-LE and SMOOTH. The mean ice area and ice volume and loss trends over the central Arctic are not consistently or significantly different between simulations in any seasons (Figure 6, Figures S3 and S4 in Supporting Information S1). To further assess how changes in feedbacks or processes in SMOOTH might affect the sea ice, we calculate the ice season, or total days per year with sea ice cover, at each grid point in the central Arctic by summing the number of days that there is an ice concentration above 15%. We analyze the distribution of ice season length by decade for both the ensemble means and for the individual ensemble members; by analyzing decades we are better able to evaluate a range of

Table 1
2020–2100 Linear Trend and Coefficient of Determination

	CESM2-LE Autumn	CESM2-LE Winter	CESM2-LE Spring	CESM2-LE Summer	SMOOTH Autumn	SMOOTH Winter	SMOOTH Spring	SMOOTH Summer
10 m wind speed								
Trend (cm s^{-1} decade $^{-1}$)	14.3	6.3	0.6	3.1	9.1	5.8	-2.0	-0.2
r^2 (unitless)	0.98	0.82	0.09	0.7	0.7	0.4	0.06	0.0
Temperature gradient								
Trend ($^{\circ}\text{C}$ decade $^{-1}$)	-0.77	-0.67	0.25	0.37	-0.75	-0.63	0.24	0.36
r^2 (unitless)	0.98	0.95	0.97	0.99	0.95	0.85	0.74	0.9
Surface temperature								
Trend ($^{\circ}\text{C}$ decade $^{-1}$)	1.75	1.43	0.36	0.27	1.69	1.41	0.34	0.26
r^2 (unitless)	1.0	0.97	0.98	0.98	0.97	0.91	0.87	0.94
925 hPa temperature								
Trend ($^{\circ}\text{C}$ decade $^{-1}$)	1.75	1.43	0.36	0.27	0.94	0.78	0.59	0.63
r^2 (unitless)	1.0	0.97	0.98	0.98	0.97	0.87	0.91	0.95
Surface wind stress								
Trend ((m N m^2) decade $^{-1}$)	0.2	0.5	0.0	0.0	0.3	0.3	-0.5	-0.1
r^2 (unitless)	0.22	0.46	0.04	0.0	0.04	0.04	0.1	0.02
Total turbulent flux								
Trend ((W m^2) decade $^{-1}$)	2.69	1.44 ^a	-0.24	-0.83	2.61	1.38 ^a	-0.15	-0.79
r^2 (unitless)	1.0	0.84 ^a	0.9	0.99	0.96	0.76 ^a	0.3	0.9
Sensible heat flux								
Trend ((W m^2) decade $^{-1}$)	0.52	0.82 ^a	-0.13	-0.33	0.52	0.79 ^a	-0.07	-0.33
r^2 (unitless)	0.91	0.88 ^a	0.81	0.98	0.82	0.79 ^a	0.12	0.88
Latent heat flux								
Trend ((W m^2) decade $^{-1}$)	2.17	0.63 ^a	-0.12	-0.50	2.08	0.59 ^a	-0.08	-0.46
r^2 (unitless)	1.0	0.78 ^a	0.92	0.99	0.96	0.69 ^a	0.43	0.88

Note. The linear trends and coefficients of determination correspond to the dashed linear trend lines shown on Figures 3, 9, and 11.

^aAs seen in Figure 9, the trends for these values are not well represented by a linear trend. The values are provided in this table for completeness but should be treated with caution.

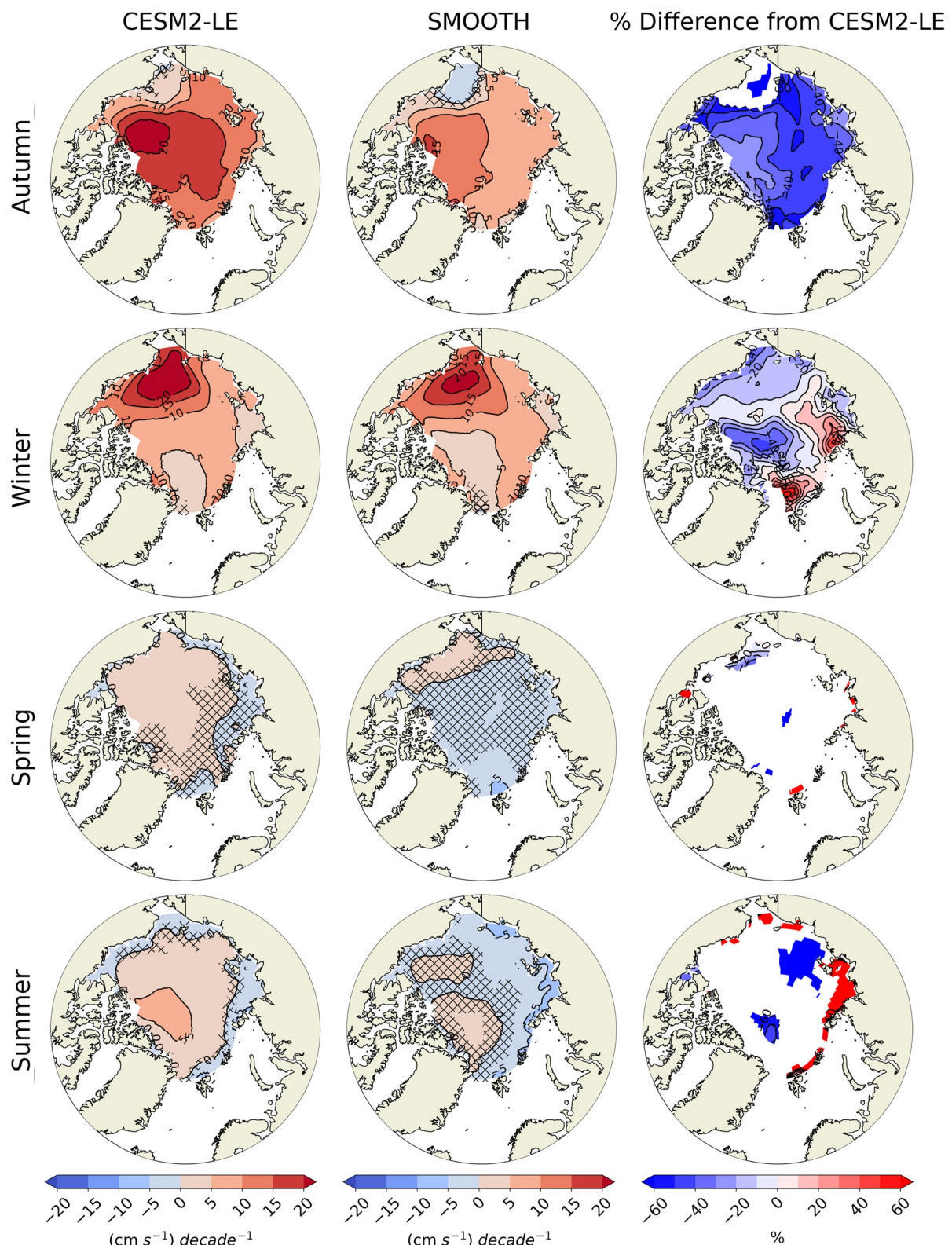


Figure 4. Ensemble mean 2020–2100 10 m wind speed linear trends ($(\text{m s}^{-1}) \text{ decade}^{-1}$) for autumn (top row), winter (second row), spring (third row), and summer (bottom row) for CESM2-LE (left column), SMOOTH (middle column), and percent difference (right column) in SMOOTH from CESM2-LE. For CESM2-LE and SMOOTH, trends that are significant at the 95% level do not have hatching, and the percent differences are only shown for locations where both trends are statistically significant—note that very large percent differences are primarily due to small CESM2-LE trend values in the difference calculation.

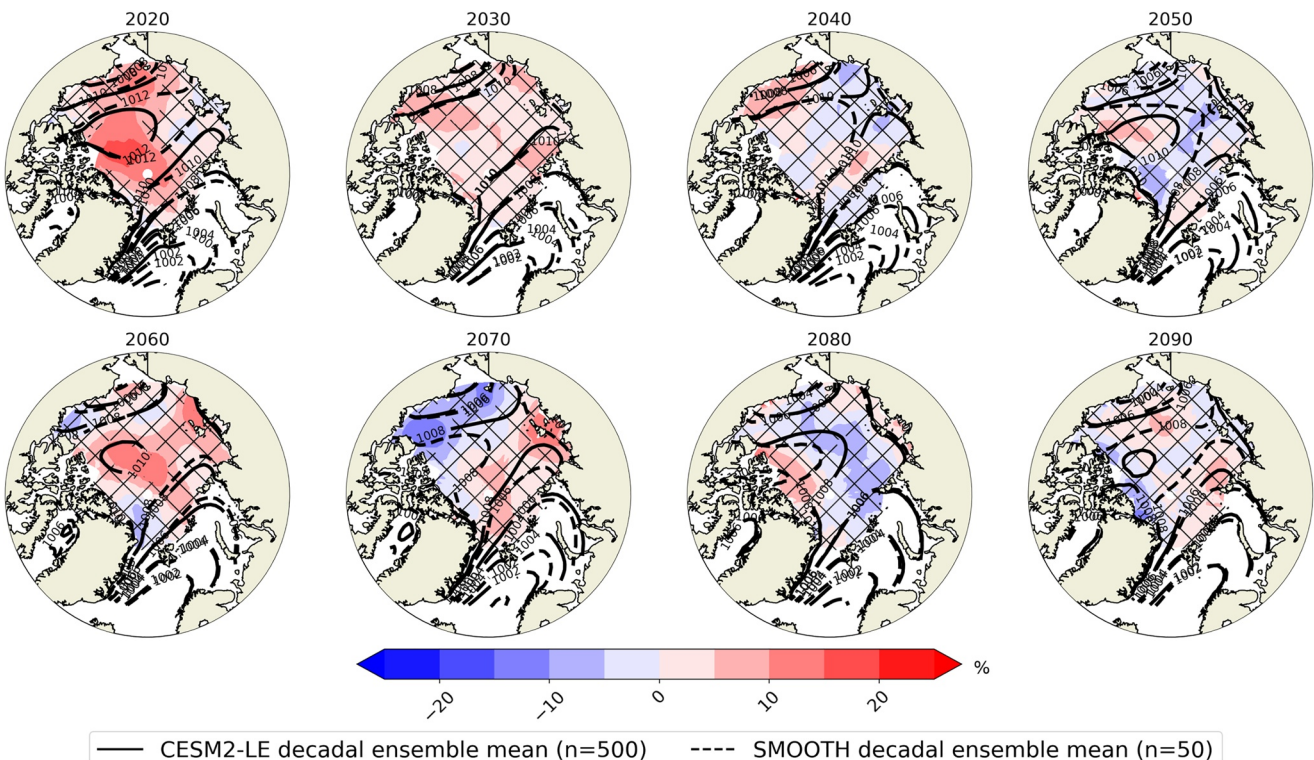


Figure 5. Autumn (OND) mean geostrophic wind speed differences (%) and sea level pressure (hPa) over decades 2020–2090. Percent differences in geostrophic wind speed at 925 hPa for SMOOTH from CESM2-LE for each decade are shown in colors and the sea level pressure for CESM2-LE (solid black) and SMOOTH (dotted black) are overlaid. Differences in 925 hPa geostrophic wind speed that are significant at the 95% level do not have hatching. Decadal means are averaged over all years and all ensemble members in the given decade ($n = 500$ for CESM2-LE; $n = 50$ for SMOOTH).

possible ice conditions due to internal climate variability. The distribution of median and lower and upper quartile ice season by decade for both the ensemble means and the individual ensemble members is nearly identical (Figure 7) and there are not any consistent spatial differences across the central Arctic (Figure S5 in Supporting Information S1). Thus, changing surface roughness does not alter feedbacks or processes in any way that drives significant impacts on the sea ice area and volume mean state or trends in any season or any region of the Arctic. These results showing no statistically significant changes in the sea ice extent and volume with smoother ice differ from Rae et al. (2014), which found that in the HadGEM3 model the sea ice state was significantly impacted with increases in surface ice roughness.

However, the surface smoothing does have a significant impact on the ice motion. In order to average ice speeds over the same ice-covered area each decade we show ice motion in March since the total ice area does not change significantly over the 21st century in this month (Figure S4a in Supporting Information S1). We find that the sea ice circulation patterns are similar in CESM2-LE and SMOOTH, and they both have the anticyclonic Beaufort Gyre and the Transpolar Drift from the Siberian Coast through the Fram Strait (Figures 8a and 8b, Figure S6 in Supporting Information S1). The mean ice speeds are lower by $>10\%$ in SMOOTH compared to CESM2-LE over much of the central Arctic (Figure 8c and Figure S6 in Supporting Information S1). Since the atmospheric circulation is so similar between CESM2-LE and SMOOTH in all seasons (Figure 5 and Figure S2 in Supporting Information S1), we do not believe that differences in the ice motion in SMOOTH are related to changes in atmospheric circulation or cyclone activity. Instead, it appears the ice circulation patterns are simply slower in SMOOTH than CESM2-LE but the circulation pattern itself is not significantly different. Over the central Arctic, the mean ice speeds in SMOOTH are about 1 cm s^{-1} lower than in CESM2-LE, though there is an increasing ice speed trend of similar magnitude in both CESM2-LE ($0.25 \text{ (cm s}^{-1}\text{)/decade}$) and SMOOTH ($0.23 \text{ (cm s}^{-1}\text{)/decade}$) (Figure 8d). While the ice speeds are different, the ice mass fluxes from the central Arctic are not significantly different in CESM2-LE and SMOOTH (Figure S7 in Supporting Information S1) and therefore changes in sea ice dynamics do not drive mean state differences.

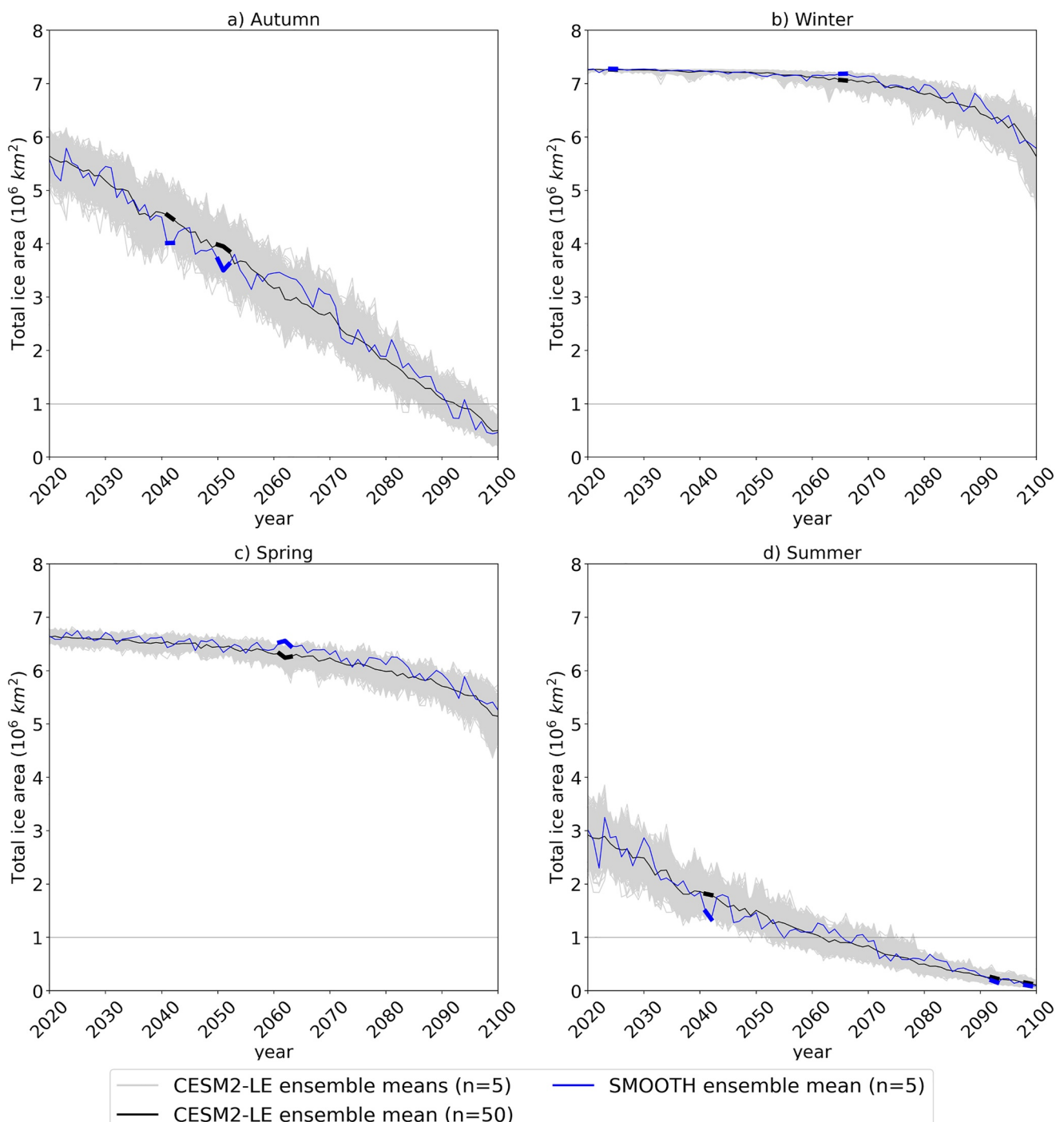


Figure 6. CESM2-LE and SMOOTH central Arctic average total sea ice area (km^2) time series for (a) autumn, (b) winter, (c) spring, (d) summer. Blue solid lines indicate SMOOTH ensemble mean ($n = 5$), black solid lines indicate CESM2-LE ensemble mean ($n = 50$), and gray solid lines indicate 1000 CESM2-LE bootstrapped ensemble means ($n = 5$). The blue and black solid lines are thick for years in which the differences are significant at the 95% confidence level.

3.3. Surface Fluxes

We have identified that there is an impact of the changing surface roughness on wind speed and ice speed, but not on sea ice state. Because near-surface winds are an essential component to coupled surface momentum and heat flux exchanges, we now examine surface fluxes in CESM2-LE and SMOOTH. The mean surface wind stress is slightly lower, particularly in the winter and spring seasons, for SMOOTH than CESM2-LE, and there

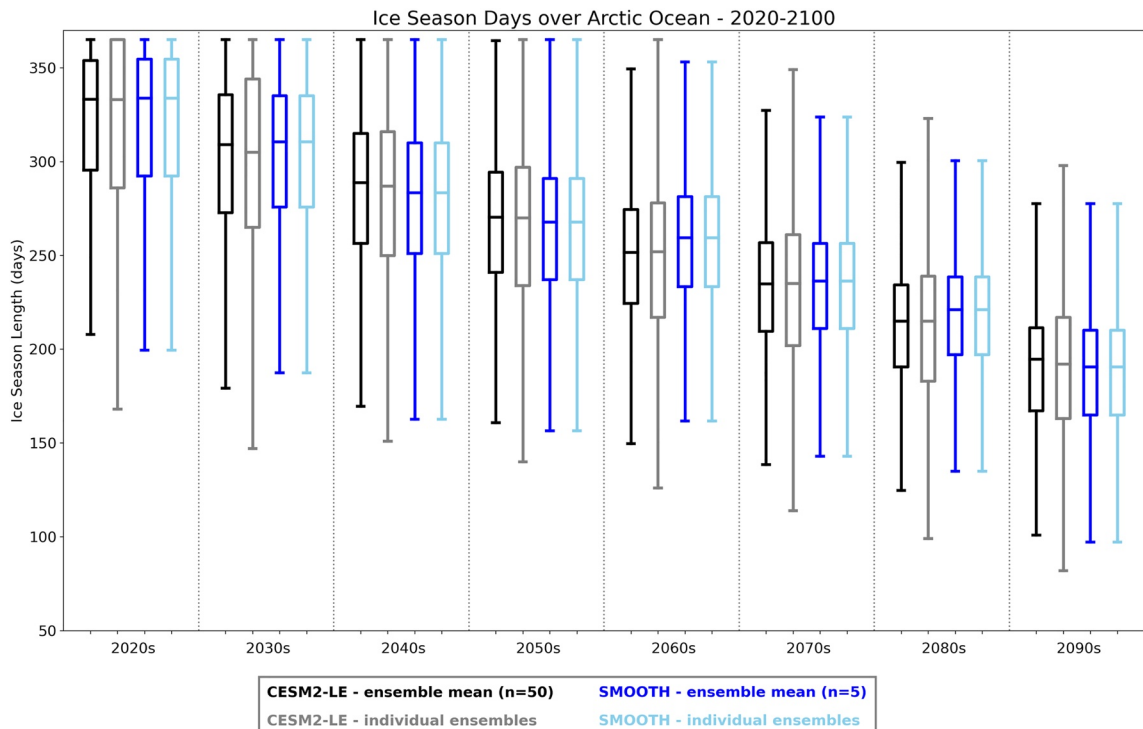


Figure 7. CESM2-LE and SMOOTH central Arctic distribution of number of ice season days by decade. Ice season distributions are calculated for all years within a decade and at all spatial points in the central Arctic for the CESM2-LE and SMOOTH ensemble means (black and dark blue, respectively) and for all ensemble members (gray and light blue, respectively). For the ensemble means, both CESM2-LE and SMOOTH have the same sample size ($n = 10$), while for the individual ensemble members the sample sizes differ between CESM2-LE ($n = 500$) and SMOOTH ($n = 50$).

are not significant linear trends in any season (Figure 9 and Table 1). It is important to note that while the winter and spring surface stress are consistently lower in SMOOTH, they are not statistically different from CESM2-LE in most years. This result is surprising because we found significantly faster wind speeds and slower ice speeds in SMOOTH compared to CESM2-LE, which are both consistent with a decrease in momentum flux from the atmosphere to the ice. We propose that the lack of significance in the surface stress differences may be due to two factors. First, if the surface stress is more variable than wind or ice speeds, then the smaller ensemble size for SMOOTH makes it more difficult to determine significant differences in surface stress. Second, there may be compensation between decreased surface roughness and increased wind strength (Equation 4) in SMOOTH that leads to a muted surface stress response. Nonetheless, the lower surface wind stress in SMOOTH is consistent with both the higher mean wind speeds (Figure 3) and lower mean ice speeds (Figure 8), and it implies that with the artificially smooth surface there is less momentum being transferred from the atmosphere to the sea ice.

In all seasons, the total turbulent heat flux is positive indicating that the atmosphere is gaining energy from the surface. In most seasons, the turbulent heat fluxes are very similar in both CESM2-LE and SMOOTH (Figure 9). The exception is spring, when SMOOTH has consistently lower latent heat flux over the central Arctic, though the differences are not statistically significant in most years. We propose that, as for surface stress, there may be compensation between higher wind speeds and decreased transfer coefficients due to the decreased roughness. The result is that artificially smoothing the ice surface in SMOOTH does not have a significant impact on surface heat fluxes.

3.4. Stability

As discussed in Section 1, a third factor that could drive near-surface wind speed increases in the Arctic is decreasing stability that could result in more momentum mixed downward to the surface from the free troposphere. We investigate whether near-surface stability differs in the experiments due to the imposed surface roughness differences. We use the atmospheric temperature gradient between 925 hPa and the surface as a proxy

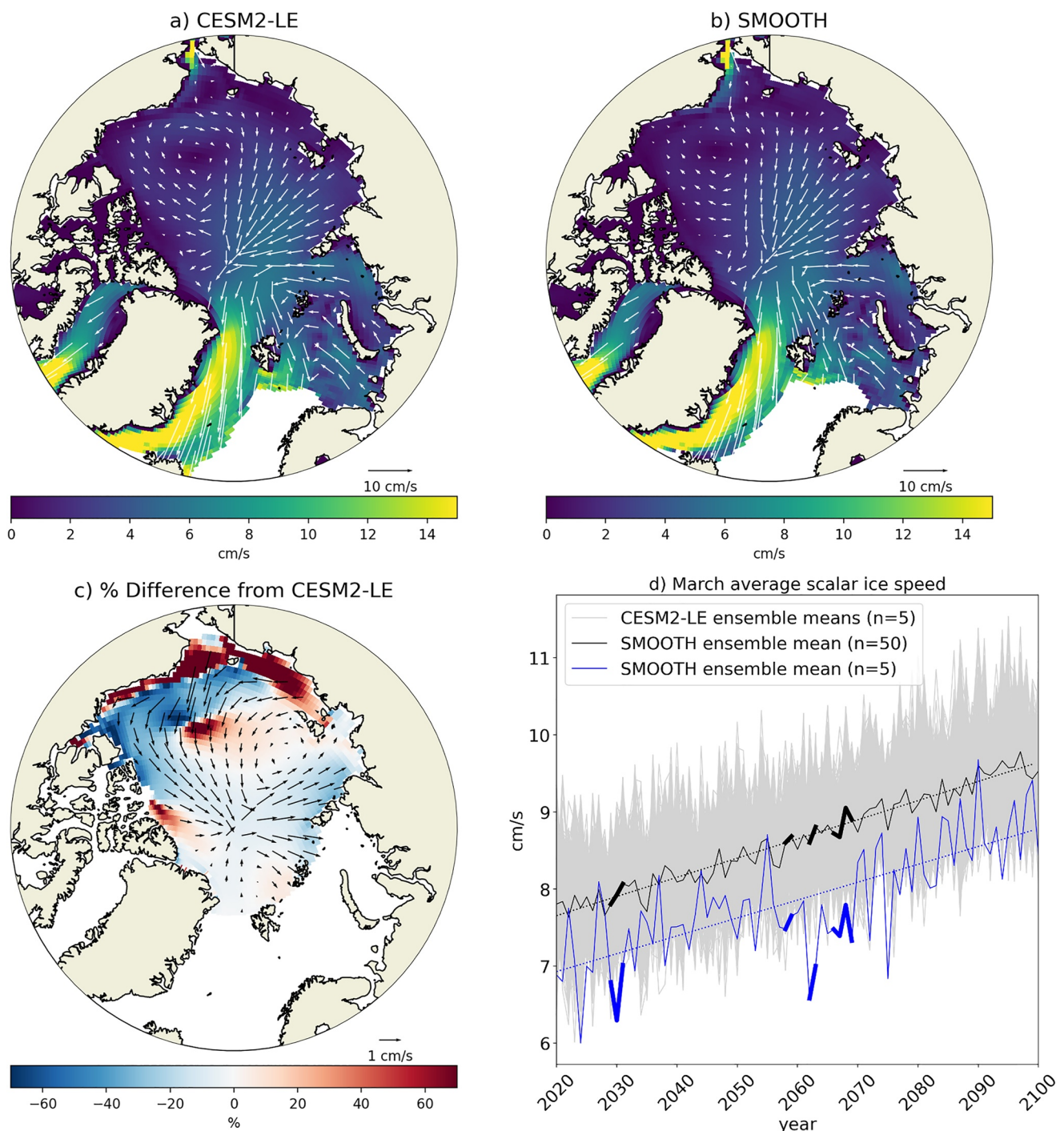


Figure 8. March sea ice circulation and speed (cm s^{-1}) for (a) CESM2-LE, (b) SMOOTH, and (c) percent difference SMOOTH from CESM2-LE in the 2020s, and (d) time series of mean scalar ice speed over the central Arctic. In panels (a)–(c), the colors indicate scalar ice speeds and vectors indicate direction. In panel d, blue solid lines indicate SMOOTH ensemble mean ($n = 5$), black solid lines indicate CESM2-LE ensemble mean ($n = 50$), and gray solid lines indicate 1000 CESM2-LE bootstrapped ensemble means ($n = 5$). The blue and black solid lines are thick for years in which the differences are significant at the 95% confidence level. Linear regressions for the ensemble means from 2020 to 2100 are shown as blue and black dashed lines.

for near-surface stability. Other Arctic atmospheric stability studies have often used the 850 hPa pressure level (e.g., de Boer et al., 2012; Medeiros et al., 2011; Schweiger et al., 2008), but we wanted to focus as near the surface as possible so use a lower pressure level. We also examined the temperature gradient between 850 hPa and the surface and the results were similar to what we found at 925 hPa and are not shown here. A negative

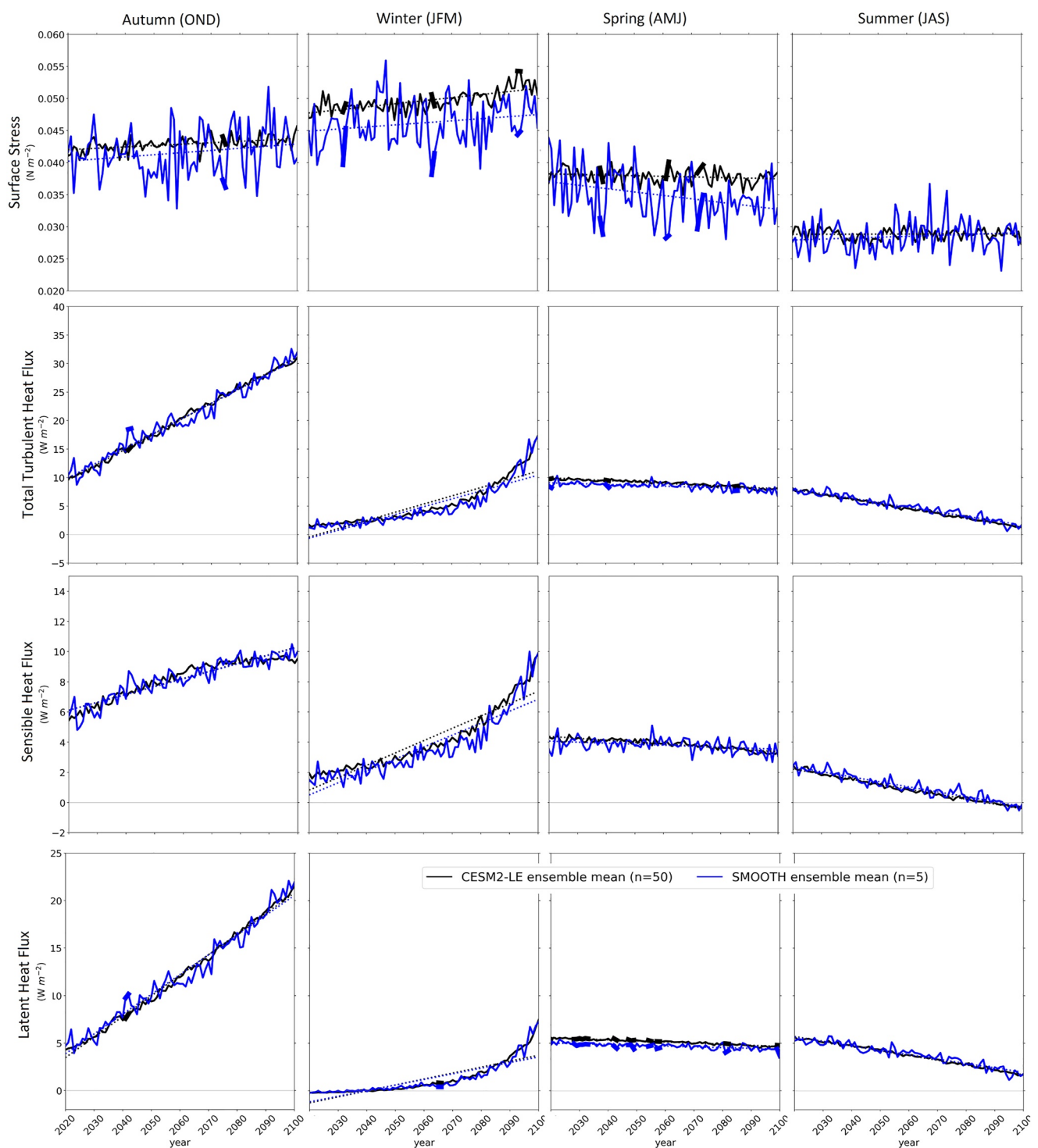


Figure 9. CESM2-LE and SMOOTH central Arctic surface flux time series for surface stress (N m^{-2} ; top row), total turbulent heat flux (W m^{-2} ; second row), sensible heat flux (W m^{-2} ; third row), and latent heat flux (W m^{-2} ; bottom row) for autumn (left column), winter (second column), spring (third column), and summer (right column). Blue solid lines indicate SMOOTH ensemble mean ($n = 5$) and black solid lines indicate CESM2-LE ensemble mean ($n = 50$). The blue and black solid lines are thick for years in which the differences are significant at the 95% confidence level.

temperature gradient indicates unstable atmospheric conditions, and a negative trend in temperature gradient indicates the atmosphere is becoming more unstable over time. We find that across the central Arctic the trends in near-surface temperature gradients are strongly negative, indicating increasingly unstable conditions, in autumn

and winter, though differences between CESM2-LE and SMOOTH are $<10\%$ over most of the region (Figure 10). The increasingly unstable conditions in autumn and winter would contribute constructively to the impact of changing surface roughness, and act to increase mixing of momentum downward from the free troposphere such that the near-surface winds would increase. In contrast, in spring and summer, the temperature gradient trends are positive, though small in magnitude, indicating that the atmosphere is becoming slightly more stable in these seasons and increasing wind speeds are likely not due to changing stability as the stability trends would inhibit downward transfer of momentum from the free troposphere.

The signs and magnitudes of the temperature gradient trends are very similar in CESM2-LE and SMOOTH, which indicates that imposed surface roughness differences do not strongly affect the stability contribution to wind speed trends. As can be seen in Figure 11, in all seasons, the central Arctic mean temperature gradient and temperatures at the surface and aloft are not significantly different between experiments. The increasing instability during ice growth seasons is driven by surface temperature increases rather than temperature changes at 925 hPa, while in the ice melt seasons, the atmosphere becomes more stable because the rate of temperature increase is higher aloft than at the surface (Figure 11 and Table 1). Indeed, the linear trends in temperature at 925 hPa remain relatively constant through the year, but the surface trends differ more through the year because they are directly related to the changing surface and sea ice loss. Our findings are consistent with others who have found that the changing sea ice surface is the primary driver for stability changes in the Arctic (Taylor et al., 2015; Watkins, 2022).

4. Discussion

In SMOOTH, with an artificially imposed smooth surface and no decrease in surface roughness over the 21st century, the mean wind speeds are higher and the increasing wind speed trends are 30%–60% lower in autumn and winter compared to the CESM2-LE. Previous studies have shown a strong connection between near-surface wind trends and sea ice loss over the historical period (e.g., Jakobson et al., 2019). For future climates, near-surface winds are strongly negatively correlated with the sea ice concentration (CESM2-LE), but removing the impact of decreasing surface roughness that would occur with ice loss (SMOOTH) the negative correlations become significantly weaker (Figure 12). The strong relationship between the sea ice and the winds seen in the CESM2-LE correlations is driven substantially, though not entirely, by the surface roughness contribution of sea ice to the changing winds because removing the roughness contribution weakens the relationship. Thus, because surface roughness impacts projected Arctic wind trends, it is important to better understand how surface roughness may change in the future. Observed sea ice roughness varies due to ice conditions including concentration, thickness, ridge fraction, pond fraction, etc. (e.g., Lüpkes et al., 2013), yet models, including CESM2, often use a single constant that can vary across models by an order of magnitude or more (Jakobson et al., 2019; Valkonen et al., 2021). While sea ice generally has a rougher surface than open water (Martin et al., 2014), at least one CMIP model even has increasing surface roughness with ice loss (Vavrus & Alkama, 2021). Experiments with variable ice roughness have found that there is a decline in sea ice roughness purely associated with the transition from multiyear ice to first year ice and the associated surface conditions (Martin et al., 2016). The impact of the transition to more first year ice on surface roughness is not something we are able to consider in this study because of the simple parameterization in CICE, but this effect may be important. It is possible that a more realistic surface roughness scheme might result in a larger influence on surface winds because in addition to the ice and ocean roughness contrast there would be a change in the ice roughness itself due to the changing ice state. An interesting question is whether it is realistic to expect decreasing roughness length in reality over sea ice as the concentration decreases. Indeed, observations over the marginal ice zone indicate that the surface roughness reaches a maximum at concentrations between 0.6 and 0.8 (Elvidge et al., 2016; Lüpkes et al., 2012), so uniformly smoother ice, as we test in this study, may not be realistic until much lower ice concentrations exist in the Arctic. There have been a number of recent efforts to observe sea ice roughness (e.g., Elvidge et al., 2016, 2021), particularly over the marginal ice zone, using a variety of methods (Gupta et al., 2014; Petty et al., 2017; Srivastava et al., 2022), and there has been progress in developing new parameterizations of surface roughness (Elvidge et al., 2016, 2021; Lüpkes et al., 2012; Tsamados et al., 2014). Indeed, several studies with coupled forecast models and more complex surface roughness treatments have shown improvements in near-surface wind speeds (Elvidge et al., 2023; Renfrew et al., 2019; Schneider et al., 2022; Thomas et al., 2021). Other studies have highlighted the importance of improving parameterizations including form drag for improving forecasting in the Arctic (Ortega et al., 2022; Ponsoni et al., 2021). Therefore, employing more sophisticated surface roughness

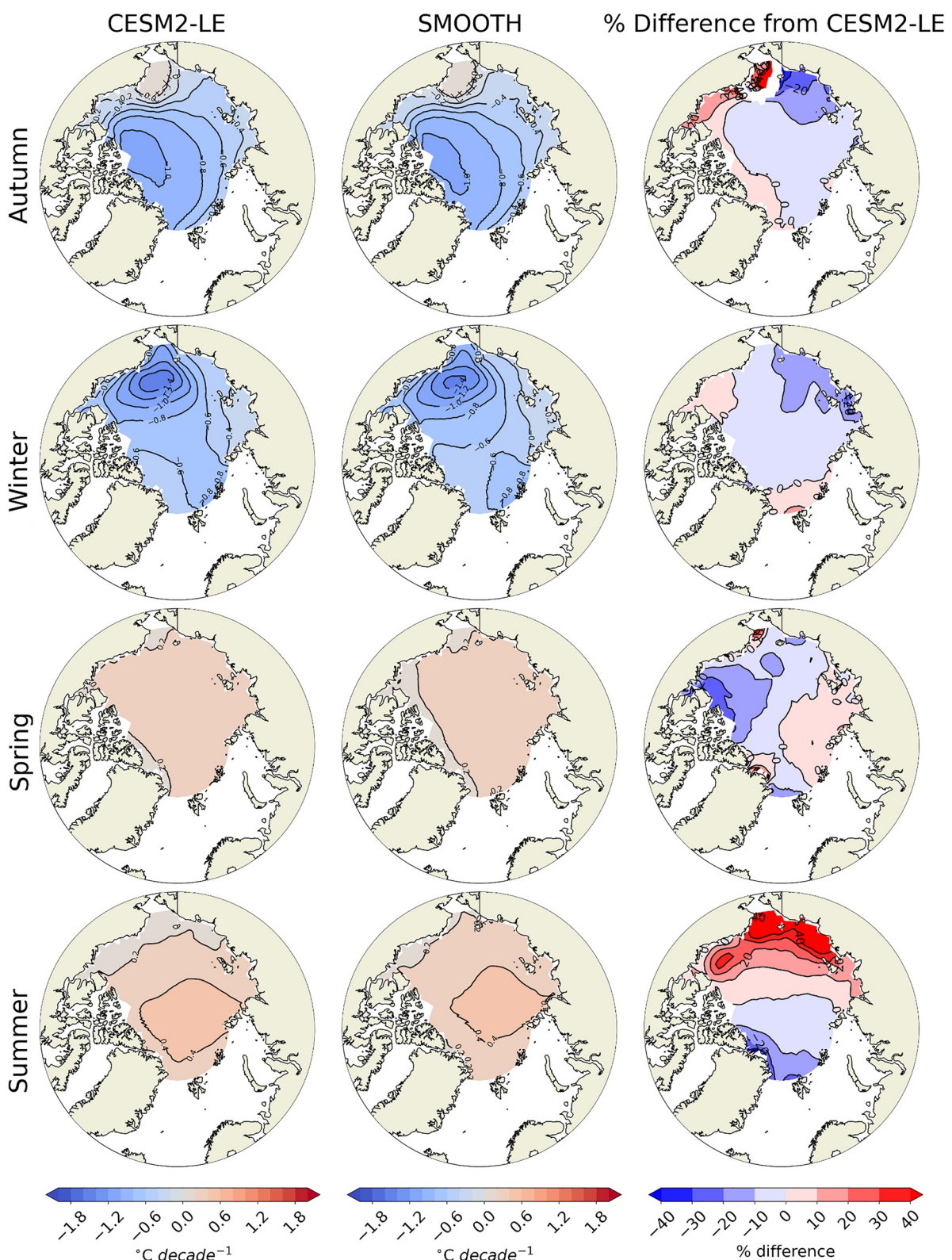


Figure 10. Ensemble mean 2020–2100 vertical temperature gradient linear trends ($^{\circ}\text{C decade}^{-1}$) for autumn (top row), winter (second row), spring (third row), and summer (bottom row) for CESM2-LE (left column), SMOOTH (middle column), and percent difference (right column) in SMOOTH from CESM2-LE. The vertical temperature gradient is defined as the temperature difference at the 925 hPa atmospheric pressure level minus the surface temperature ($T_{925 \text{ hPa}} - T_{\text{fc}}$). For CESM2-LE and SMOOTH, trends that are significant at the 95% level do not have hatching, and the percent differences are only shown for locations where both trends are statistically significant.

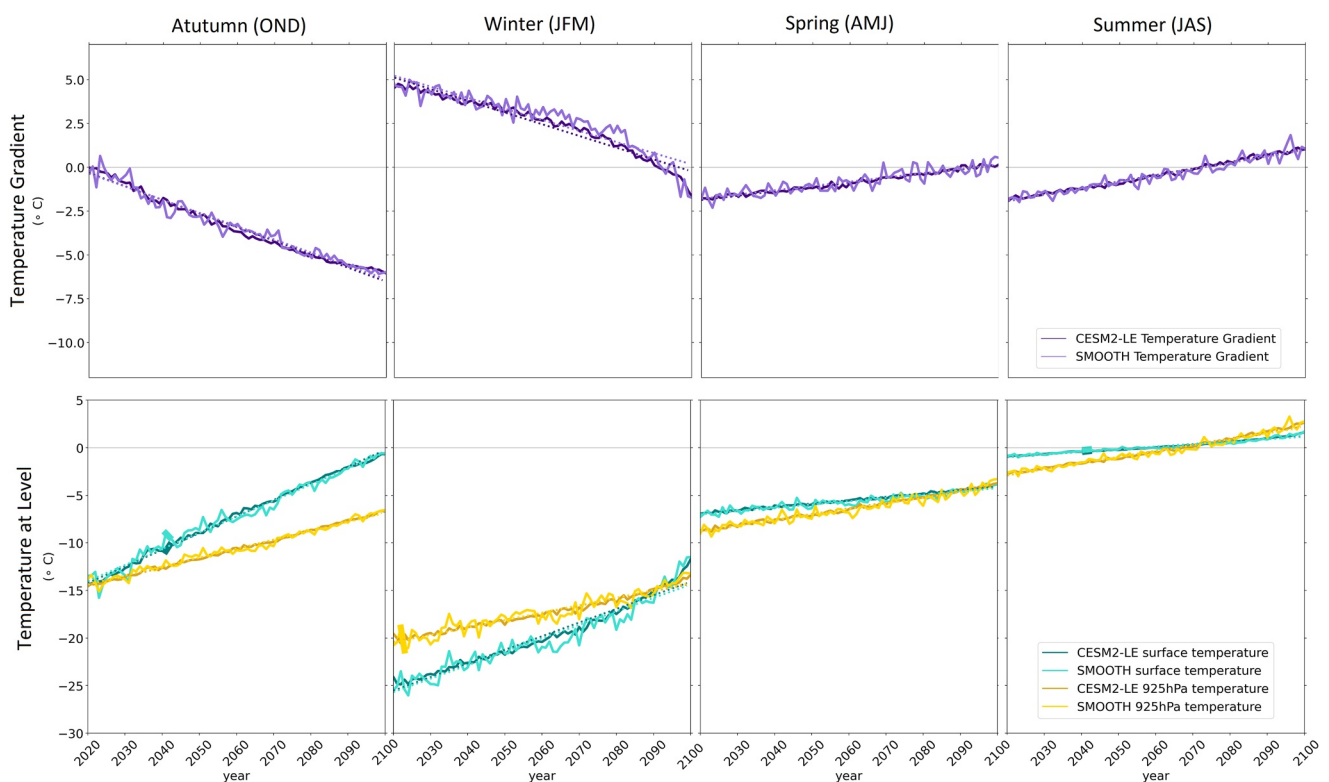


Figure 11. CESM2-LE and SMOOTH central Arctic: temperature gradient (top row; $^{\circ}\text{C}$) and temperature at the surface and 925 hPa (bottom row; $^{\circ}\text{C}$) time series for autumn (left column), winter (second column), spring (third column), summer (right column). Temperature gradient is defined as the temperature difference at the 925 hPa atmospheric pressure level minus the surface temperature ($T_{925\text{ hPa}} - T_{\text{fc}}$). Solid lines indicate SMOOTH ensemble mean ($n = 5$) and CESM2-LE ensemble mean ($n = 50$) for: temperature gradient (purple, left column), surface temperature (green, right column), and 925 hPa temperature (gold, right column) where the darker shade of each color indicates CESM2-LE and the lighter shade indicates SMOOTH. The lines are thick for years in which the differences are significant at the 95% confidence level. Linear regressions for the ensemble means from 2020 to 2100 are shown as dashed lines.

parameterizations in state-of-the-art coupled earth system models that run for 10–100 s of years in different ice and ocean conditions could impact climate projections of near-surface winds.

Interestingly, it seems the combination of changing roughness and atmospheric stability trends determine the sign of the near-surface wind trends. We find that CESM2-LE and SMOOTH have nearly identical temperature gradient trends and that in the ice growth season the atmosphere becomes more unstable due to a rapid increase in surface temperatures as initiation of freeze up occurs later in the year. In contrast, in the ice melt season, the atmosphere becomes slightly more stable, and this is due to faster rates of increasing temperatures aloft than at the surface. The less stable atmosphere in the ice growth season would enhance wind speeds, but in the ice melt season the more stable atmosphere should suppress wind speeds. In all seasons, CESM2-LE has predominantly increasing near-surface wind speeds, consistent with other studies (Mioduszewski et al., 2018; Vavrus & Alkama, 2021). In contrast, during the ice melt season, when the atmosphere is becoming more stable, SMOOTH has a negative near-surface wind trend. Because CESM2-LE does not have a negative winds speed trend in the ice melt season, it is likely that the decreasing surface roughness is especially important for setting the sign of the wind speed increase in these months.

While there is a clear response of the mean wind speed and trends to the surface conditions, the changing surface condition appears to drive little difference in the sea ice. The sea ice mean state and trends for ice area, ice volume, and ice season length are very similar for both SMOOTH and CESM2-LE. There is a strong relationship between global average CO_2 and total sea ice area for both autumn and spring that is nearly identical in both the CESM2-LE and SMOOTH (Figure 13). This strong relationship between greenhouse gas emissions is consistent with observational studies (Notz & Stroeve, 2016). The similar relationship between CO_2 and sea ice area in both experiments indicates that there are not significant feedbacks between the surface conditions that impact the sea ice state, but instead the sea ice is driven primarily from the large-scale Arctic warming due to increasing greenhouse gasses.

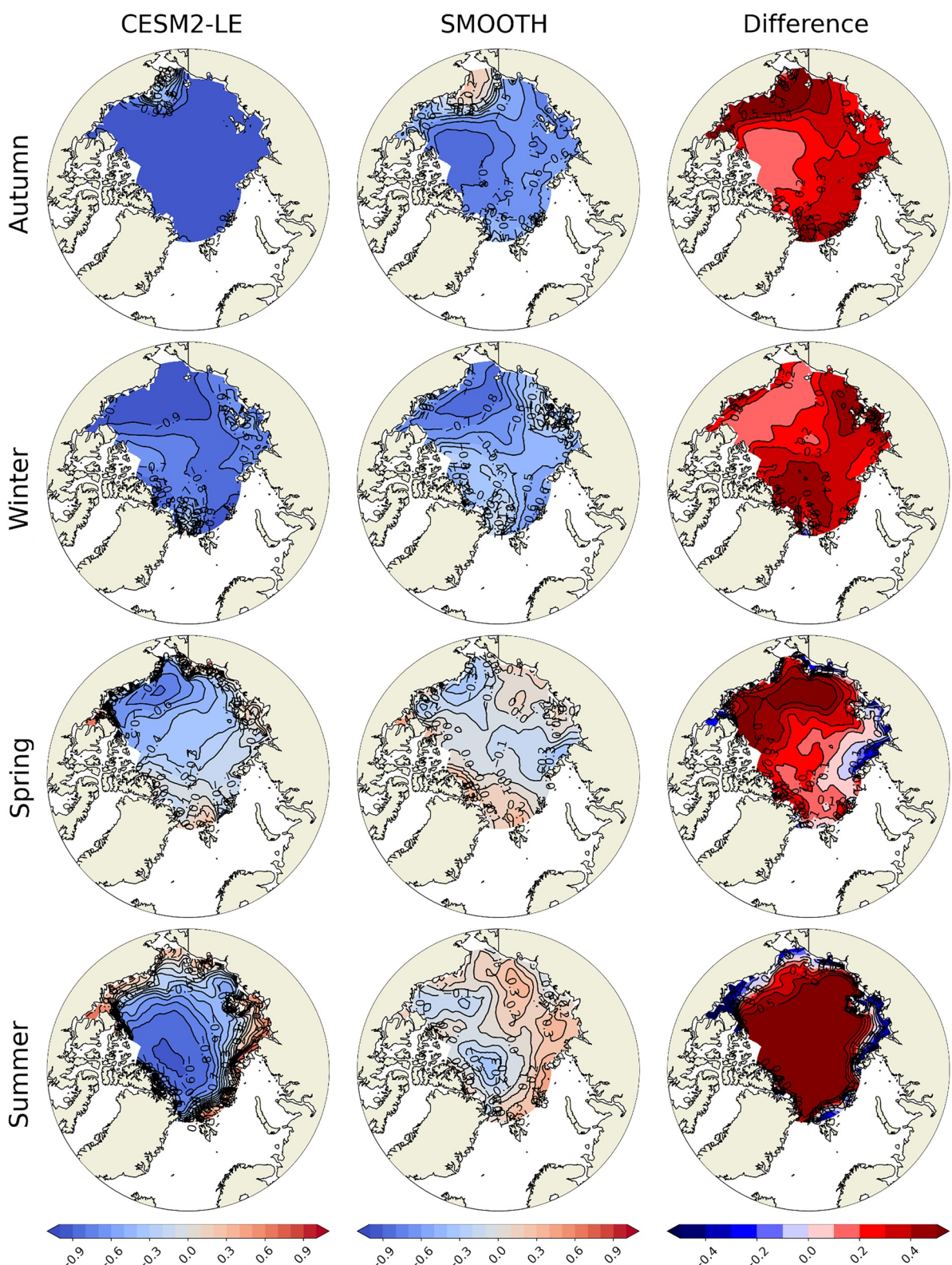


Figure 12. Correlation coefficient between ensemble mean 2020–2100 10-m wind speed and sea ice concentration for autumn (top row), winter (second row), spring (third row), and summer (bottom row) for CESM2-LE (left column), SMOOTH (middle column), and difference (right column; SMOOTH-CESM2-LE).

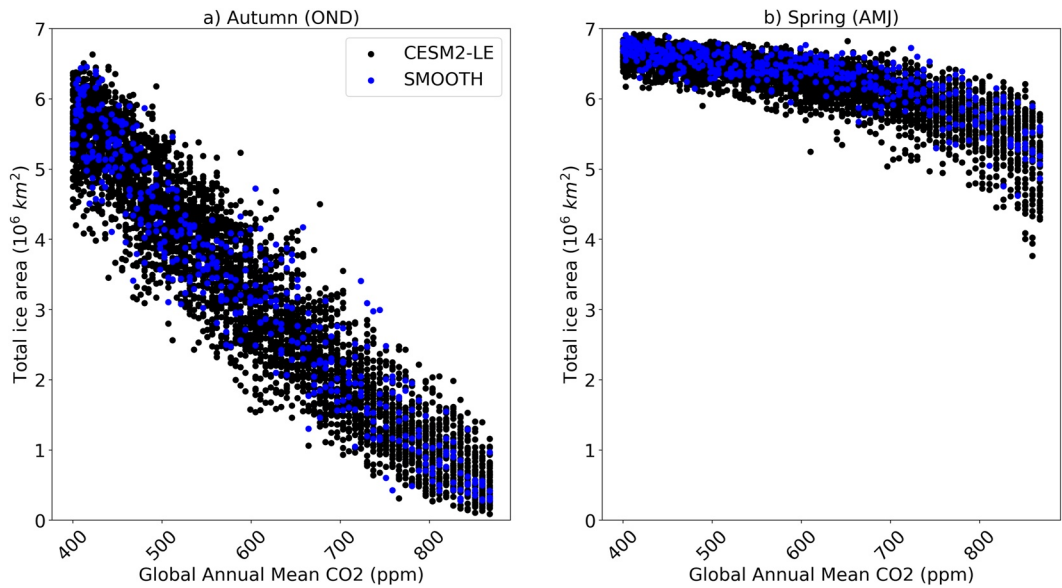


Figure 13. Global mean CO₂ concentration and total seasonal Arctic sea ice area for (a) autumn and (b) spring. CO₂ values are annual means for the period 2015–2100. Values for all CESM2-LE (50) and SMOOTH (5) ensemble members are shown.

The only major difference from roughness that we found for sea ice was related to the sea ice speeds. Compared to CESM2-LE, SMOOTH has faster mean near-surface wind speeds and slower ice speeds, particularly in winter. All other inputs remaining the same, a faster wind speed would be expected to drive a larger momentum flux (Equation 4). So, the decrease in surface stress in SMOOTH despite the faster wind speeds indicates there is likely compensation between lower surface roughness and the faster winds. Lower surface stress results in less momentum being transferred from the atmosphere to the surface, so the wind speeds are higher and ice speeds lower. It is important to note that the differences in surface wind stress are not statistically significant over much of the 21st century (Figure 9), and this may be related to the compensation between roughness and wind speed or the larger variability in SMOOTH due to the small ensemble size. Future work with a larger ensemble could clarify the magnitude of the roughness impact on surface momentum flux.

Differences in surface momentum flux have been proposed drivers of feedbacks with ocean mixing and ice transport that could impact the sea ice mean state. Observational studies have shown that ocean mixing from strong winds can lead to sea ice loss (J. Zhang et al., 2013), yet in our study there is not a difference in ice loss despite the difference in mean wind speeds between experiments. Another possible feedback from the reduced momentum flux would be through impacts on ice transport. We do find that there are lower ice speeds in SMOOTH, but the overall ice mass fluxes are not significantly different between the experiments. This may be due to the shift toward a seasonal ice cover in the Arctic, so dynamic drivers of ice state become less relevant than thermodynamic drivers when there is more first year ice that melts the following summer (Krumpen et al., 2019). Additionally, there is not a significant trend in surface wind stress over the 21st century, while both the wind and ice speed trends are positive over time. The projected positive ice speed trend is consistent with observations of faster ice motion in recent years (Rampal et al., 2009; Spreen et al., 2011; F. Zhang et al., 2021). Faster ice speeds have often been attributed to thinner ice that has reduced ice strength, but ice motion may also be increasing due to increasing wind speed. However, in this study, we cannot disentangle the impacts of changing ice strength and wind speeds on sea ice speed trends.

There are not significant differences in surface heat fluxes in the two experiments other than in spring for latent heat flux, which we will discuss shortly. A possible explanation for the negligible differences in surface heat fluxes is that in SMOOTH there is a compensating relationship between the increased winds due to the decreased momentum flux and a lower exchange coefficient due to decreased surface roughness. The temperature conditions are not significantly different (Figure 11), which implies that the wind and exchange coefficient impacts must roughly compensate leading to statistically indistinguishable surface heat in CESM2-LE and SMOOTH. In spring, the latent heat flux is smaller over the entire central Arctic in SMOOTH than CESM2-LE despite similar

ice areal extent and ice volume. Even though there are faster winds in SMOOTH during this season that could drive higher latent heat flux, it is not immediately apparent why there is not compensation with the exchange coefficient in this season only. Other studies have found that there is active coupling between sea ice and the atmosphere in spring (Huang et al., 2019). Thus, the differences in evaporation due to changed surface roughness could, theoretically, lead to a feedback response with longwave radiation reaching the ice surface. Yet we do not see indications that there are differences in ice extent or thickness in winter or spring (Figure 6, Figures S3, and S4 in Supporting Information S1), so this wind-evaporation-radiation feedback does not appear to significantly impact ice state in our experiment. Indeed, the surface heat fluxes reflect how similarly the sea ice evolves because starting in the 2070s in winter there is sharp, nonlinear increase in the surface turbulent fluxes for both experiments (Figure 9), and this is likely due to a thinning of the sea ice in both CESM2-LE and SMOOTH to such a degree that there are larger wintertime fluxes of heat from the ocean to atmosphere through the sea ice (Landrum & Holland, 2021).

5. Conclusions

The goal of this study was to address how changing surface roughness due to sea ice loss impact the Arctic climate using coupled Earth system model experiments, and below we summarize answers to the questions posed in the introduction:

- *What are the relative contributions of changing surface roughness and boundary layer stability to the projected increasing wind speeds?* Without a general decrease in roughness over the 21st century associated with sea ice loss, the wind speed trends are 30%–60% smaller in autumn and winter than in the experiments where surface roughness evolves over time with changing sea ice cover. Changes in stability are likely responsible for the rest of the wind speed trends. Therefore, during the two seasons in which positive Arctic wind speed trends are strongest, our results suggest that stability is primarily responsible for the strengthening surface winds, but reduced surface roughness also plays a significant role and can be comparable in importance in some seasons and regions. Additionally, we find that without a decrease in surface roughness the signs of the small wind trends in spring and summer differ from the experiments where surface conditions affect roughness. Thus, the combination of roughness and stability changes due to changing sea ice state over the 21st century are both essential for driving the sign and magnitude of the projected wind speed trends. Thus, it might be important to adjust the stability correction functions to observations over sea ice as the ones proposed by Grachev et al. (2007) or Grynkiv et al. (2020).
- *Does changing surface roughness have any coupled impacts that contribute to Arctic sea ice loss or affect turbulent fluxes?* Sea ice state and trends are driven by warming temperature and surface roughness changes and their coupled impacts do not impact sea ice state. Surface roughness has modest impacts the surface momentum flux, but impacts on turbulent heat fluxes are insignificant.

In short, the near-surface wind trends are the result of how sea ice loss drives changes in both surface roughness and near-surface atmospheric stability, yet the sea ice mean state and trends are not driven by coupled impacts from surface roughness on near-surface winds or fluxes but from the overall warming trend due to increasing greenhouse gas emissions. Because the Arctic wind trends do depend on surface roughness, it is important to better understand how surface roughness may change in the future by using more sophisticated and realistic representations of surface roughness in coupled models.

Data Availability Statement

The CESM2-LE data used in this study are freely available, as described in Rodgers et al. (2021). The SMOOTH model experiments were run using the CESM Polar Climate Working Group allocation, and data are freely available online (A. DuVivier et al., 2023). The computational notebooks and other data processing tools used for this publication are freely available online (A. DuVivier, 2023).

Acknowledgments

AKD wrote the main manuscript text, prepared the figures, and ran the model experiments. MMH, SJV, LL, CAS, and RT contributed to the model experimental design, provided feedback throughout the analysis process, and reviewed the manuscript. All authors acknowledge appreciate support for this work from the National Science Foundation (NSF) Award 2043588. CAS also acknowledges support from the U.S. Department of Energy, Office of Science, Office of Biological & Environmental Research (BER), Regional and Global Model Analysis (RGMA) component of the Earth and Environmental System Modeling Program under Award Number DE-SC0022070 and NSF IA 1947282. This material is based upon work supported by the National Center for Atmospheric Research (NCAR), which is a major facility sponsored by NSF under Cooperative Agreement 1852977. The CESM project is supported primarily by NSF. Computing and data storage resources, including the Cheyenne supercomputer (Computational and Information Systems Laboratory, 2017), were provided by the Computational and Information Systems Laboratory (CISL) at NCAR. We thank all the scientists, software engineers, and administrators who contributed to the development of CESM2.

References

Aksenov, Y., Popova, E. E., Yool, A., Nurser, A. G., Williams, T. D., Bertino, L., & Bergh, J. (2016). On the future navigability of Arctic sea routes: High-resolution projections of the Arctic Ocean and sea ice. *Marine Policy*, 75, 300–317. <https://doi.org/10.1016/j.marpol.2015.12.027>

Alkama, R., Koffi, E. N., Vavrus, S. J., Diehl, T., Francis, J. A., Stroeve, J., et al. (2020). Wind amplifies the polar sea ice retreat. *Environmental Research Letters*, 15(12), 124022. <https://doi.org/10.1088/1748-9326/abc379>

Ashjian, C. J., Braund, S. R., Campbell, R. G., George, J. C., Kruse, J., Maslowski, W., et al. (2010). Climate variability, oceanography, bowhead whale distribution, and Inupiat subsistence whaling near Barrow, Alaska. *Arctic*, 63(2), 179–194. <https://doi.org/10.14430/arctic973>

Assur, A. (1958). Arctic sea ice. In *Chap. Composition of sea ice and its tensile strength* (pp. 106–138). National Academy of Sciences-National Research Council.

Barnhart, K. R., Anderson, R. S., Overeem, I., Wobus, C., Clow, G. D., & Urban, F. E. (2014). Modeling erosion of ice-rich permafrost bluffs along the Alaskan Beaufort Sea coast. *Journal of Geophysical Research: Earth Surface*, 119, 1155–1179. <https://doi.org/10.1002/2013JF002845>

Computational and Information Systems Laboratory. (2017). *Cheyenne: SGI ICE XA cluster*. UCAR/NCAR. <https://doi.org/10.5065/D6RX99HX>

Danabasoglu, G., Lamarque, J., Bacmeister, J., Bailey, D. A., DuVivier, A. K., Edwards, J., et al. (2020). The Community Earth System Model Version 2 (CESM2). *Journal of Advances in Modeling Earth Systems*, 12, e2019MS001916. <https://doi.org/10.1029/2019MS001916>

de Boer, G., Chapman, W., Kay, J. E., Medeiros, B., Shupe, M. D., Vavrus, S., & Walsh, J. (2012). A characterization of the present-day Arctic atmosphere in CCSM4. *Journal of Climate*, 25(8), 2676–2695. <https://doi.org/10.1175/JCLI-D-11-00228.1>

DeRepentigny, P., Jahn, A., Holland, M. M., & Smith, A. (2020). Arctic sea ice in two configurations of the Community Earth System Model Version 2 (CESM2) during the 20th and 21st centuries. *Journal of Geophysical Research: Oceans*, 125, e2020JC016133. <https://doi.org/10.1029/2020JC016133>

Dobrynin, M., Murawsky, J., & Yang, S. (2012). Evolution of the global wind wave climate in CMIP5 experiments. *Geophysical Research Letters*, 39, L18606. <https://doi.org/10.1029/2012GL052843>

DuVivier, A. (2023). CESM2 SMOOTH analysis scripts. *Zenodo*. <https://doi.org/10.5281/zenodo.8299658>

DuVivier, A., Vavrus, S., Holland, M., Landrum, L., Shields, C., & Thaker, R. (2023). CESM2 SMOOTH experiments. UCAR/NCAR-GDEX. <https://doi.org/10.5065/gc1-kg59>

DuVivier, A. K., Holland, M. M., Kay, J. E., Tilmes, S., Gettelman, A., & Bailey, D. A. (2020). Arctic and Antarctic sea ice mean state in the Community Earth System Model Version 2 and the influence of atmospheric chemistry. *Journal of Geophysical Research: Oceans*, 125, e2019JC015934. <https://doi.org/10.1029/2019JC015934>

Elvidge, A. D., Renfrew, I. A., Brooks, I. M., Srivastava, P., Yelland, M. J., & Prytherch, J. (2021). Surface heat and moisture exchange in the marginal ice zone: Observations and a new parameterization scheme for weather and climate models. *Journal of Geophysical Research: Atmospheres*, 126, e2021JD034827. <https://doi.org/10.1029/2021JD034827>

Elvidge, A. D., Renfrew, I. A., Edwards, J. M., Brooks, I. M., Srivastava, P., & Weiss, A. I. (2023). Improved simulation of the polar atmospheric boundary layer by accounting for aerodynamic roughness in the parameterization of surface scalar exchange over sea ice. *Journal of Advances in Modeling Earth Systems*, 15, e2022MS003305. <https://doi.org/10.1029/2022MS003305>

Elvidge, A. D., Renfrew, I. A., Weiss, A. I., Brooks, I. M., Lachlan-Cope, T. A., & King, J. C. (2016). Observations of surface momentum exchange over the marginal ice zone and recommendations for its parametrization. *Atmospheric Chemistry and Physics*, 16(3), 1545–1563. <https://doi.org/10.5194/acp-16-1545-2016>

Grachev, A. A., Andreas, E. L., Fairall, C. W., Guest, P. S., & Persson, P. O. G. (2007). SHEBA flux-profile relationships in the stable atmospheric boundary layer. *Boundary-Layer Meteorology*, 124(3), 315–333. <https://doi.org/10.1007/s10546-007-9177-6>

Gryanik, V. M., Lüpkes, C., Grachev, A., & Sidorenko, D. (2020). New modified and extended stability functions for the stable boundary layer based on SHEBA and parametrizations of bulk transfer coefficients for climate models. *Journal of the Atmospheric Sciences*, 77(8), 2687–2716. <https://doi.org/10.1175/JAS-D-19-0255.1>

Gupta, M., Barber, D. G., Scharien, R. K., & Isleifson, D. (2014). Detection and classification of surface roughness in an arctic marginal sea ice zone: Surface roughness in MIZ. *Hydrological Processes*, 28(3), 599–609. <https://doi.org/10.1002/hyp.9593>

Huang, Y., Dong, X., Bailey, D. A., Holland, M. M., Xi, B., DuVivier, A. K., et al. (2019). Thicker clouds and accelerated Arctic sea ice decline: The atmosphere-sea ice interactions in spring. *Geophysical Research Letters*, 46, 6980–6989. <https://doi.org/10.1029/2019GL082791>

Hunke, E. C., Lipscomb, W. H., Turner, A. K., Jeffery, N., & Elliott, S. (2015). *Cice: The Los Alamos sea ice model documentation and software user's manual version 5* (Technical Report). Los Alamos National Laboratory.

Jahn, A., Kay, J. E., Holland, M. M., & Hall, D. M. (2016). How predictable is the timing of a summer ice-free Arctic? *Geophysical Research Letters*, 43, 9113–9120. <https://doi.org/10.1002/2016GL070067>

Jakobson, L., Vihma, T., & Jakobson, E. (2019). Relationships between sea ice concentration and wind speed over the arctic ocean during 1979–2015. *Journal of Climate*, 32(22), 7783–7796. <https://doi.org/10.1175/JCLI-D-19-0271.1>

Kay, J. E., DeRepentigny, P., Holland, M. M., Bailey, D. A., DuVivier, A. K., Blanchard-Wrigglesworth, E., et al. (2022). Less surface sea ice melt in the CESM2 improves Arctic sea ice simulation with minimal non-polar climate impacts. *Journal of Advances in Modeling Earth Systems*, 14, e2021MS002679. <https://doi.org/10.1029/2021MS002679>

Kay, J. E., Raeder, K., Gettelman, A., & Anderson, J. (2011). The boundary layer response to recent Arctic sea ice loss and implications for high-latitude climate feedbacks. *Journal of Climate*, 24(2), 428–447. <https://doi.org/10.1175/2010JCLI3651.1>

Keen, A., Blockley, E., Bailey, D. A., Boldingh Debernard, J., Bushuk, M., Delhay, S., et al. (2021). An inter-comparison of the mass budget of the Arctic sea ice in CMIP6 models. *The Cryosphere*, 15(2), 951–982. <https://doi.org/10.5194/tc-15-951-2021>

Khon, V. C., Mokhov, I. I., Pogarskiy, F. A., Babanin, A., Dethloff, K., Rinke, A., & Matthes, H. (2014). Wave heights in the 21st century Arctic Ocean simulated with a regional climate mode. *Geophysical Research Letters*, 41, 2956–2961. <https://doi.org/10.1002/2014GL059847>

Knippertz, P., Ulbrich, U., & Speth, P. (2000). Changing cyclones and surface wind speeds over the North Atlantic and Europe in a transient GHG experiment. *Climate Research*, 15, 109–122. <https://doi.org/10.3354/cr015109>

Krumpen, T., Belter, H. J., Boetius, A., Damm, E., Haas, C., Hendricks, S., et al. (2019). Arctic warming interrupts the Transpolar Drift and affects long-range transport of sea ice and ice-rafted matter. *Scientific Reports*, 9(1), 5459. <https://doi.org/10.1038/s41598-019-41456-y>

Kwok, R. (2018). Arctic sea ice thickness, volume, and multiyear ice coverage: Losses and coupled variability (1958–2018). *Environmental Research Letters*, 13(10), 105005. <https://doi.org/10.1088/1748-9326/aae3ec>

Landrum, L., & Holland, M. M. (2021). Influences of changing sea ice and snow thicknesses on Arctic winter heat fluxes. *The Cryosphere*, 1–16. <https://doi.org/10.5194/tc-2021-245>

Large, W. G., & Yeager, S. G. (2009). The global climatology of an interannually varying air-sea flux data set. *Climate Dynamics*, 33(2–3), 341–364. <https://doi.org/10.1007/s00382-008-0441-3>

Lecomte, O., Fichefet, T., Flocço, D., Schroeder, D., & Vancoppenolle, M. (2015). Interactions between wind-blown snow redistribution and melt ponds in a coupled ocean–sea ice model. *Ocean Modelling*, 87, 67–80. <https://doi.org/10.1016/j.ocemod.2014.12.003>

Lüpkes, C., Grynkiv, V. M., Hartmann, J., & Andreas, E. L. (2012). A parametrization, based on sea ice morphology, of the neutral atmospheric drag coefficients for weather prediction and climate models. *Journal of Geophysical Research*, 117, D13112. <https://doi.org/10.1029/2012JD017630>

Lüpkes, C., Grynkiv, V. M., Rösel, A., Birnbaum, G., & Kaleschke, L. (2013). Effect of sea ice morphology during Arctic summer on atmospheric drag coefficients used in climate models. *Geophysical Research Letters*, 40, 446–451. <https://doi.org/10.1002/grl.50081>

Martin, T., Steele, M., & Zhang, J. (2014). Seasonality and long-term trend of Arctic Ocean surface stress in a model. *Journal of Geophysical Research: Oceans*, 119, 1723–1738. <https://doi.org/10.1002/2013JC009425>

Martin, T., Tsamados, M., Schroeder, D., & Feltham, D. L. (2016). The impact of variable sea ice roughness on changes in Arctic Ocean surface stress: A model study. *Journal of Geophysical Research: Oceans*, 121, 1931–1952. <https://doi.org/10.1002/2015JC011186>

McInnes, K. L., Erwin, T. A., & Bathols, J. M. (2011). Global Climate Model projected changes in 10 m wind speed and direction due to anthropogenic climate change. *Atmospheric Science Letters*, 12(4), 325–333. <https://doi.org/10.1002/asl.341>

Medeiros, B., Deser, C., Tomas, R. A., & Kay, J. E. (2011). Arctic inversion strength in climate models. *Journal of Climate*, 24(17), 4733–4740. <https://doi.org/10.1175/2011JCLI3968.1>

Meier, W. N., Perovich, D. K., Farrell, S. L., Haas, C., Hendricks, S., Petty, A., et al. (2022). Sea ice [in “state of the climate in 2021”]. *Bulletin of the American Meteorological Society*, 103(8), S270–S273. <https://doi.org/10.1175/BAMS-D-22-0082.1>

Melia, N., Haines, K., & Hawkins, E. (2016). Sea ice decline and 21st century trans-Arctic shipping routes: Trans-Arctic shipping in the 21st century. *Geophysical Research Letters*, 43, 9720–9728. <https://doi.org/10.1002/2016GL069315>

Mioduszewski, J., Vavrus, S., & Wang, M. (2018). Diminishing Arctic sea ice promotes stronger surface winds. *Journal of Climate*, 31(19), 8101–8119. <https://doi.org/10.1175/JCLI-D-18-0109.1>

Notz, D., & Community, S. (2020). Arctic sea ice in CMIP6. *Geophysical Research Letters*, 47, e2019GL086749. <https://doi.org/10.1029/2019GL086749>

Notz, D., & Stroeve, J. (2016). Observed Arctic sea-ice loss directly follows anthropogenic CO₂ emission. *Science*, 354(6313), 747–750. <https://doi.org/10.1126/science.aag2345>

Ortega, P., Blockley, E. W., Køltzow, M., Massonnet, F., Sandu, I., Svensson, G., et al. (2022). Improving arctic weather and seasonal climate prediction: Recommendations for future forecast systems evolution from the European project APPLICATE. *Bulletin of the American Meteorological Society*, 103(10), E2203–E2213. <https://doi.org/10.1175/BAMS-D-22-0083.1>

Petty, A. A., Tsamados, M. C., & Kurtz, N. T. (2017). Atmospheric form drag coefficients over Arctic sea ice using remotely sensed ice topography data, spring 2009–2015. *Journal of Geophysical Research: Earth Surface*, 122, 1472–1490. <https://doi.org/10.1002/2017JF004209>

Ponsoni, L., Gupta, M., Sterlin, J., Massonnet, F., Fichefet, T., Hinrichs, C., et al. (2021). Deliverable No. 2.5 final report on model developments and their evaluation in coupled mode (Technical Report). *Zenodo*. <https://doi.org/10.5281/ZENODO.4916934>

Rae, J., Hewitt, H., Keen, A., Ridley, J., Edwards, J., & Harris, C. (2014). A sensitivity study of the sea ice simulation in the global coupled climate model, HadGEM3. *Ocean Modelling*, 74, 60–76. <https://doi.org/10.1016/j.ocemod.2013.12.003>

Rampal, P., Weiss, J., & Marsan, D. (2009). Positive trend in the mean speed and deformation rate of Arctic sea ice, 1979–2007. *Journal of Geophysical Research*, 114, C05013. <https://doi.org/10.1029/2008JC005066>

Redilla, K., Pearl, S. T., Bieniek, P. A., & Walsh, J. E. (2019). Wind climatology for Alaska: Historical and future. *Atmospheric and Climate Sciences*, 9(04), 683–702. <https://doi.org/10.4236/acs.2019.94042>

Renfrew, I. A., Elvidge, A. D., & Edwards, J. M. (2019). Atmospheric sensitivity to marginal-ice-zone drag: Local and global responses. *Quarterly Journal of the Royal Meteorological Society*, 145(720), 1165–1179. <https://doi.org/10.1002/qj.3486>

Rodgers, K. B., Lee, S.-S., Rosenbloom, N., Timmermann, A., Danabasoglu, G., Deser, C., et al. (2021). Ubiquity of human-induced changes in climate variability. *Earth System Dynamics*, 12(4), 1393–1411. <https://doi.org/10.5194/esd-12-1393-2021>

Rousset, C., Vancoppenolle, M., Madec, G., Fichefet, T., Flavoni, S., Barthélémy, A., et al. (2015). The Louvain-La-Neuve sea ice model LIM3.6: Global and regional capabilities. *Geoscientific Model Development*, 8(10), 2991–3005. <https://doi.org/10.5194/gmd-8-2991-2015>

Ruosteenoja, K., Vihma, T., & Venäläinen, A. (2019). Projected changes in European and north Atlantic seasonal wind climate derived from CMIP5 simulations. *Journal of Climate*, 32(19), 6467–6490. <https://doi.org/10.1175/JCLI-D-19-0023.1>

Schneider, T., Lüpkes, C., Dorn, W., Chechin, D., Handorf, D., Khosravi, S., et al. (2022). Sensitivity to changes in the surface-layer turbulence parameterization for stable conditions in winter: A case study with a regional climate model over the arctic. *Atmospheric Science Letters*, 23(1), e1066. <https://doi.org/10.1002/asl.1066>

Schweiger, A. J., Lindsay, R. W., Vavrus, S., & Francis, J. A. (2008). Relationships between Arctic sea ice and clouds during autumn. *Journal of Climate*, 21(18), 4799–4810. <https://doi.org/10.1175/2008JCLI2156.1>

Seo, H., & Yang, J. (2013). Dynamical response of the Arctic atmospheric boundary layer process to uncertainties in sea-ice concentration. *Journal of Geophysical Research: Atmospheres*, 118, 12383–12402. <https://doi.org/10.1002/2013JD020312>

Spreen, G., Kwok, R., & Menemenlis, D. (2011). Trends in Arctic sea ice drift and role of wind forcing: 1992–2009. *Geophysical Research Letters*, 38, L19501. <https://doi.org/10.1029/2011GL048970>

Srivastava, P., Brooks, I. M., Prytherch, J., Salisbury, D. J., Elvidge, A. D., Renfrew, I. A., & Yelland, M. J. (2022). Ship-based estimates of momentum transfer coefficient over sea ice and recommendations for its parameterization. *Atmospheric Chemistry and Physics*, 22(7), 4763–4778. <https://doi.org/10.5194/acp-22-4763-2022>

Stegall, S. T., & Zhang, J. (2012). December wind field climatology, changes, and extremes in the Chukchi–Beaufort seas and Alaska north slope during 1979–2009. *Journal of Climate*, 25(23), 8075–8089. <https://doi.org/10.1175/JCLI-D-11-00532.1>

Stevenson, T. C., Davies, J., Huntington, H. P., & Sheard, W. (2019). An examination of trans-Arctic vessel routing in the Central Arctic Ocean. *Marine Policy*, 100, 83–89. <https://doi.org/10.1016/j.marpol.2018.11.031>

Taylor, P. C., Kato, S., Xu, K.-M., & Cai, M. (2015). Covariance between Arctic sea ice and clouds within atmospheric state regimes at the satellite footprint level. *Journal of Geophysical Research: Atmospheres*, 120, 12656–12678. <https://doi.org/10.1002/2015JD023520>

Thomas, E. E., Müller, M., Bohlinger, P., Batrak, Y., & Szapiro, N. (2021). A kilometer-scale coupled atmosphere-wave forecasting system for the European Arctic. *Weather and Forecasting*, 36, 2087–2099. <https://doi.org/10.1175/WAF-D-21-0065.1>

Tsamados, M., Feltham, D. L., Schroeder, D., Flocço, D., Farrell, S. L., Kurtz, N., et al. (2014). Impact of variable atmospheric and oceanic form drag on simulations of Arctic sea ice. *Journal of Physical Oceanography*, 44(5), 1329–1353. <https://doi.org/10.1175/JPO-D-13-0215.1>

Valkonen, E., Cassano, J., & Cassano, E. (2021). Arctic cyclones and their interactions with the declining sea ice: A recent climatology. *Journal of Geophysical Research: Atmospheres*, 126, e2020JD034366. <https://doi.org/10.1029/2020JD034366>

Vavrus, S. J., & Alkama, R. (2021). Future trends of arctic surface wind speeds and their relationship with sea ice in CMIP5 climate model simulations. *Climate Dynamics*, 59, 1833–1848. <https://doi.org/10.1007/s00382-021-06071-6>

Wang, X. L., Feng, Y., Swail, V. R., & Cox, A. (2015). Historical changes in the Beaufort-Chukchi-Bering seas surface winds and waves, 1971–2013. *Journal of Climate*, 28(19), 7457–7469. <https://doi.org/10.1175/JCLI-D-15-0190.1>

Waseda, T., Webb, A., Sato, K., Inoue, J., Kohout, A., Penrose, B., & Penrose, S. (2018). Correlated increase of high ocean waves and winds in the ice-free waters of the arctic ocean. *Scientific Reports*, 8(1), 4489. <https://doi.org/10.1038/s41598-018-22500-9>

Watkins, D. (2022). *Vertical structure of the lower troposphere in a changing Arctic* (Doctoral dissertation). Oregon State University. Retrieved from https://ir.library.oregonstate.edu/concern/graduate_thesis_or_dissertations/zs25xh61x

Webster, M. A., DuVivier, A. K., Holland, M. M., & Bailey, D. A. (2021). Snow on Arctic sea ice in a warming climate as simulated in CESM. *Journal of Geophysical Research: Oceans*, 126, e2020JC016308. <https://doi.org/10.1029/2020JC016308>

Yu, X., Rinke, A., Dorn, W., Spreen, G., Lüpkes, C., Sumata, H., & Grynkiv, V. M. (2020). Evaluation of Arctic sea ice drift and its dependency on near-surface wind and sea ice conditions in the coupled regional climate model HIRHAM-NAOSIM. *The Cryosphere*, 14(5), 1727–1746. <https://doi.org/10.5194/tc-14-1727-2020>

Zhang, F., Pang, X., Lei, R., Zhai, M., Zhao, X., & Cai, Q. (2021). Arctic sea ice motion change and response to atmospheric forcing between 1979 and 2019. *International Journal of Climatology*, 42(3), 1854–1876. <https://doi.org/10.1002/joc.7340>

Zhang, J., Lindsay, R., Schweiger, A., & Steele, M. (2013). The impact of an intense summer cyclone on 2012 Arctic sea ice retreat: Cyclone impact on 2012 Arctic sea ice. *Geophysical Research Letters*, 40, 720–726. <https://doi.org/10.1002/grl.50190>